AD-A059 869 PRINCETON UNIV N J DEPT OF AEROSPACE AND MECHANICAL--ETC F/G 21/9.2
BURNING RATE MEASUREMENT OF THIN SHEETS OF DOUBLE BASE PROPELLA--ETC(U)
OCT 75 L H CAVENY, C R FELSHEIM DAAA21-74-C-0332
UNCLASSIFIED AMS-1301 NL

1 OF 1
AD A059869

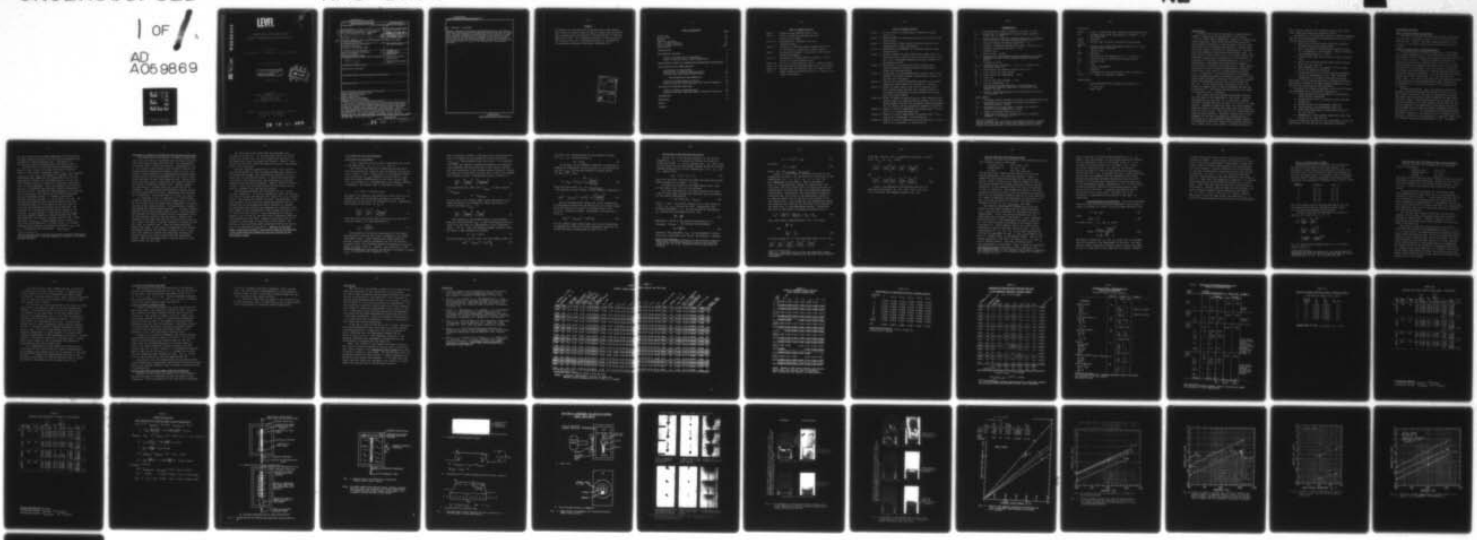

END
DATE FILMED
12-78
DDC

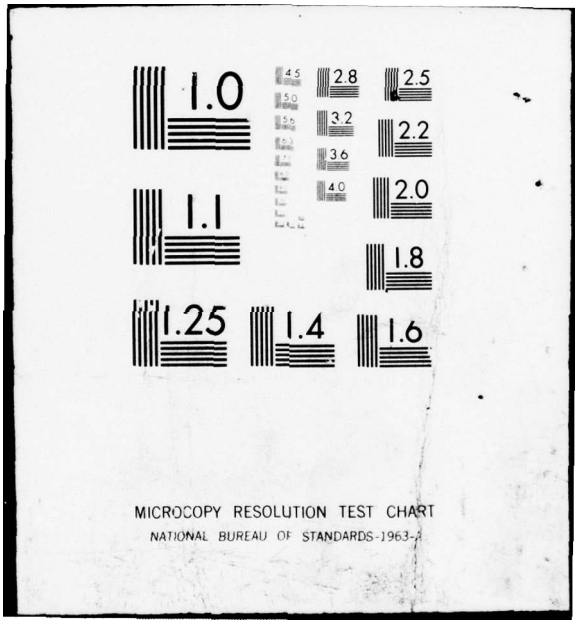
1.0
1.1
1.25
1.4
1.6
1.8
2.0
2.2
2.5
2.8
3.2
3.6
4.0
4.5
5.0
5.6
MICROCOPY RESOLUTION TEST CHART
NATIONAL BUREAU OF STANDARDS-1963-A

BURNING RATE MEASUREMENT OF THIN SHEETS OF DOUBLE BASE PROPELLANT (HEN-12)

Prepared by

L. H. Caveny, C. K. Pelsheim, and M. Summerfield

AMS REPORT NO. 1301

OCTOBER 1975

Prepared for
Product Assurance Directorate
Picatinny Arsenal
Dover, New Jersey
Under Contract DAA21-74-C-0332

Aerospace and Mechanical Sciences Department
PRINCETON UNIVERSITY
Princeton, New Jersey

SECURITY CLASSIFICATION OF THIS PAGE (When Data Entered)

REPORT DOCUMENTATION PAGE	READ INSTRUCTIONS BEFORE COMPLETING FORM
1. REPORT NUMBER	2. GOVT ACCESSION NO. 3. RECIPIENT'S CATALOG NUMBER (9)
4. TITLE (and Subtitle) (6) Burning Rate Measurement of Thin Sheets of Double Base Propellant (HEN-12)	5. TYPE OF REPORT & PERIOD COVERED Interim Rept. January to August 1975.
	6. PERFORMING ORG. REPORT NUMBER AMS REPORT-1301 (14)
7. AUTHOR(s) (10) Leonard H. Caveny, Chris R. Felsheim and Martin Summerfield	8. CONTRACT OR GRANT NUMBER(s) (15) DAAA21-74-C-0332
9. PERFORMING ORGANIZATION NAME AND ADDRESS Princeton University Princeton, New Jersey 08540	10. PROGRAM ELEMENT, PROJECT, TASK AREA & WORK UNIT NUMBERS
11. CONTROLLING OFFICE NAME AND ADDRESS Product Assurance Directorate Picatinny Arsenal Dover, New Jersey 07801 (11)	12. REPORT DATE October 1975 (12) 55 p. 13. NUMBER OF PAGES ix + 45
14. MONITORING AGENCY NAME & ADDRESS (if different from Controlling Office)	15. SECURITY CLASS. (of this report) UNCLASSIFIED 15a. DECLASSIFICATION/DOWNGRADING SCHEDULE
16. DISTRIBUTION STATEMENT (of this Report) Distribution Unlimited.	
17. DISTRIBUTION STATEMENT (of the abstract entered in Block 20, if different from Report)	
18. SUPPLEMENTARY NOTES	
19. KEY WORDS (Continue on reverse side if necessary and identify by block number) Solid propellant burning rates. Double base propellants. Sheet propellants. Strand burning techniques. Burning rate error analysis.	
20. ABSTRACT (Continue on reverse side if necessary and identify by block number) The special problems associated with determining strand burning rates of very thin (0.040 inches) sheets of an NC/NG double base propellant (specifically HEN-12) were assessed and the accuracies of several strand burning experiments were evaluated. Strand burning experiments were carried out in several media over a range of temperatures (20 to 140 F) and pressures (500 to 1500 psi): nonflowing N_2, N_2 flowing parallel to flame, water, and oil. Except for oil, all media produced consistent burning rate data.(Con'd)	

DD FORM 1 JAN 73 1473 EDITION OF 1 NOV 65 IS OBSOLETE

UNCLASSIFIED

SECURITY CLASSIFICATION OF THIS PAGE (When Data Entered)

20. Abstract - continued.

However, burning in nonflowing N_2 minimized the heat loss effects. High speed photographs and extinguished specimens showed the extent that the media retarded the burning rate of the very thin strands. Error analyses indicated that the strand burning method of using nonflowing N_2 and conventional breakwire timing of the burning period can be refined to produce errors of less than 0.5% and that the largest source of error is the determination of breakwire position.

PREFACE

The purpose of this study was to analyze and to make assessments based on several types of HEN-12 burning rate data which were obtained under the February 1975 Modification to Contract DAAA21-74-C-0332. The technical monitors for this portion of the contract were Mr. F. Bernstein and Mrs. R. Covington of the Production Assurance Directorate (SARPA-QA-A-D).

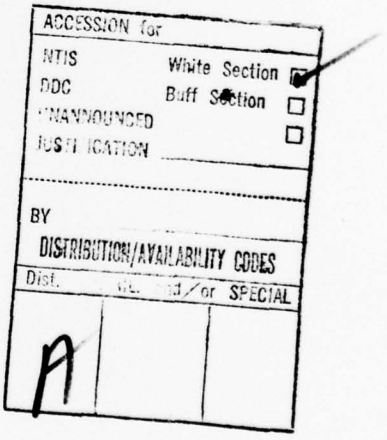

Table of Contents

LIST OF TABLE CAPTIONS

LIST OF FIGURE CAPTIONS

NOMENCLATURE*

a = pre-exponential factor in burning rate law, $r = ap^n$

C_d = coefficient of determination of the linear regression of the x_n, t_n data

C_v = coefficient of variation (standard deviation or standard error divided by the mean and multiplied by 100), %

d = distance between individual breakwires, in

L = length of propellant burned during time interval, t_b, in

n = exponent in burning rate law, $r = ap^n$

p = pressure, psi

r = burning rate, in/sec

r_{0-7} = burning rate calculated by dividing distance to farthest breakwire by time to burn through farthest breakwire, cm/sec

s = estimate of error

$s_{t \cdot x}$ = standard error estimate of t on x in terms of the regression line, sec

S_p = scale factor for pressure, psi/cm and psi/in

S_t = scale factor for time, sec/cm

S_T = scale factor for temperature, °F/in

t = time, sec

t_b = time to burn the distance L, sec

T_0 = initial temperature, °F

x = horizontal distances measured on oscilloscope and oscillograph records; positions of breakwires along strand, in, cm

y = vertical distances measured on oscilloscope and oscillograph records, cm

Greek Symbols:

δ = difference used to correct from actual to desired conditions

δr_p = adjustment in burning rate to correct from actual to desired pressure, in/sec

δr_T = adjustment in burning rate to correct from actual to desired initial temperature, in/sec

Δp = change in pressure during test, psi

σ_p = temperature sensitivity of burning rate at constant pressure, $\partial \ln r / \partial T_0)_p$, $°F^{-1}$

---

*Units of inches, psi, and °F are used rather than the SI system because those are the units which are presently used to report burning rate measurements at the Army's production facilities.

Subscripts:

actual	=	p and T_0 conditions that actually existed during test
adj	=	adjusted value which corresponds to intended p and T_0 conditions
breakw	=	breakwire
calib	=	setting used to obtain calibration oscillograph
desired, des	=	pressure and initial temperature conditions at which burning rate is desired
ig	=	igniter wire
meas	=	measured
n	=	the number of the breakwire (i.e., 1 through 7)
set	=	initial condition determined by gauge setting
std	=	standard time
t	=	time
T	=	initial temperature
p	=	pressure
1,2	=	conditions at start and finish of test respectively
0,1,2,...,7	=	number of breakwire locations

Superscripts:

^	=	value predicted from regression analysis, e.g., $\hat{t} = a_0 + a_1 x$
$\bar{}$	=	mean value

INTRODUCTION

An analytical study was undertaken to assess several methods of measuring the burning rate of thin sheets (~0.04 in. thick) HEN-12 propellant. HEN-12 is a double base, rocket propellant (about 48.0% nitrocellulose and 40.9% nitroglycerin) containing 4% finely ground lead and copper salts that serve as burning rate modifiers. Several questions have arisen concerning the uncertainties associated with three methods of measuring strand burning rates. The first method [1] (illustrated in Fig. 1a), the most widely used, determines burning rate by measuring the time required to burn past two accurately located breakwires, (i.e., a low melting point, lead based wire which melts and opens a circuit when it encounters the flame front). Flame spreading along the side of strand is prevented by coating the strand with a thin layer of a flame resistant material (i.e., an inhibitor). The second method is the chimney burner technique developed at Princeton University[2,3] which uses multiple breakwire intervals and flowing N_2 to prevent flame from spreading along the side of the strand (see Fig. 1b). In the third method (illustrated in Fig. 2), burning the strand under a liquid eliminates the need for an inhibitor[4-6]. For details on these methods, the reader is referred to Refs. 1 through 6.

Much of what has been learned from previous studies does not apply to the propellant in this study. Firstly, the propellant is very thin (i.e., 0.04 inch); whenever practical, strands should be at least 0.2 x 0.2 in. in cross section. Reference 2 points out that heat losses become a prominent source of burning rate error even for strands as large as 0.125 x 0.125. Thus, the 0.04 in. strand thickness raises serious questions. Secondly, burning rate is very dependent on the local nitroglycerin concentration and nitroglycerin in the propellant migrates rapidly whenever the propellant comes into contact with absorbent materials (e.g., paper, skin, cloth, plastic, and some inhibitors).

Thus, improper handling will introduce burning rate variations, especially when thin strands are used.

Evaluations of the production control of HEN-12 propellant lead to the following questions concerning the several burning rate measuring methods:

1) Which type of strand burning measuring technique produces the most consistent data?
2) Can a noninhibited strand produce consistent data in a nonflowing N_2 strand burner? What is affect of high temperatures, e.g., 140°F?
3) To what extent does the N_2 flow rate affect burning rate?
4) How do the following burning media affect burning rate: N_2, H_20, and oil?
5) What problems are to be expected if oil is used as the low temperature medium?
6) To what extent (if at all) do multiple breakwires reduce the experimental error? What additional information is provided by multiple wire data?

While many of the questions have been considered previously, the unusual thinness of the HEN-12 sheet propellant is the stimulus for reconsidering these questions.

To answer the foregoing questions, data from the following experiments were analyzed and interpreted:

1) Strand burning rate measurements in nonflowing N_2 using multiple breakwires.
2) Strand burning rates in flowing N_2 using multiple breakwires.
3) Strand burning rate measurement under H_20.
4) Strand burning rate measurement under oil.
5) High speed photographs of propellants burning in N_2, H_20, and oil.
6) Examination of extinguished propellants which were burning in N_2, H_20, and oil.

Particular attention was given to the experimental errors and practicality of each burning rate measuring technique.

EXPERIMENTAL APPROACH

Steps in Chimney Burner Experiments

The steps in carrying out the chimney burner experiments have been well documented in Refs. 2 and 3 and will not be repeated here. However, the data reduction method is given in detail in the section entitled Data Reduction and Error Analysis.

Steps in Burning Under Liquid Experiments

Test specimens in the form of strands were cut from the HEN-12 sheet propellant and a record was kept of the identity and location of each specimen; the specimen dimensions were about 2.06 x 0.25 x 0.04 in. Particular attention was given to controlling the accuracy (held to within ±0.002 in.) of the distance between the center of the hole for the igniter wire and the end of the specimen. For this purpose, a specially fabricated fixture was devised to hold the specimen during the cutting and drilling operations. A 0.020 inch hole was drilled through the width of the strand (i.e., the hole was 0.25 inches long). The igniter wire was 0.006 in. diameter nichrome. After preparation, the specimens were wrapped individually in aluminum foil to prevent degradation of the sample prior to testing.

The desired pressure (p_{set}) was preset by observing a pressure gauge which had been calibrated to within ±2.5 psi. The pressure rise during the test was obtained by recording the output from the Kistler 604C4 transducer and 504A charge amplifier system. (After specimen burn-out and depending on the test conditions, the final pressure may be less than the initial pressure.) The temperature of the sample and liquid were recorded using a mercury-in-glass thermometer which was calibrated to ±0.9 °F. For consistency the conditioned specimen always remained in the liquid for 120 ±5 seconds prior to ignition. Ignition was accomplished by a constant length 0.006 in. diameter nichrome wire energized by 9 VDC. Throughout

the test series the AC and RMS components of the ultra-high frequency acoustic emission from the burning propellant were recorded for future diagnostic use.* The details of the acoustic emission instrumentation are given in Ref. 6.

For each test, the following direct measurements (as shown in Figs. 2 and 3) are taken from the oscilloscope record of the pressure transducer output $y_{p,1}$, $y_{p,2}$, $y_{p,std}$, $x_{t,std}$, x_t, and t_{std}. The method for obtaining x_t was established after examining the consistency of all of the experimental records. As illustrated by Fig. 3a, the rise time following ignition is about 0.03 secs and, from test to test, is very repeatable. Also, the pressure drop following burn-out is extremely sharp and thus, gives an unambiguous end-of-test time. The burn-out time determined in this manner is very consistent with the end of the acoustic emissions which are discussed in Ref. 6. However, the acoustic emission generally precedes t_1 by as much as 0.1 sec. The distances are measured using graticule which can be read with magnification to 0.01 cm which is also the limit to which the oscilloscope photorecord can be resolved. The time base is recalculated for each test by measuring the distance ($x_{t,std}$) between a known timing interval (t_{std}). The timing marks produced by a Hewlett Packard 226A Time Mark Generator are accurate to better than 10^{-5} sec. Since the ratio $x_t/x_{t,std}$ is approximately unity, errors in scale tend to be cancelled. As shown in Fig. 3c, the mean pressure during burning is obtained by averaging $y_{p,1}$ and $y_{p,2}$ and applying the calibration, $\Delta p_{std}/y_{p,std}$.

---

*The conventional data obtained during the study were sufficiently well defined that it was not necessary to analyze the acoustic emission records.

PHOTOGRAPHIC STUDIES OF BURNING AND EXTINGUISHED PROPELLANTS

High speed movies were taken of the HEN-12 strands burning in H_2O, oil and N_2 to determine how the liquid interacts with the burning surface and flame zone. The experimental arrangement used to obtain the movies is illustrated in Fig. 4. The strand is positioned so that following ignition the burning surface traverses the camera's field of view. The strand is front-lighted by a tungsten/quartz photo-spotlight. The movies were taken with Ektachrome EF film using a Hicam Camera operating at about 2000 frames per sec. Timing marks on the film were used in conjunction with interval marks on the strands to determine burning rates. Chamber pressure was regulated by a through flow of N_2 at the top of the combustor. The strands were extinguished by rapidly venting the gas volume above the liquid. Photographs were obtained for 6 conditions: 500 psi and 1500 psi in H_2O, oil, and N_2.

As indicated in Fig. 5, specimens I3, I7 and I8 were burned at 1500 psi in H_2O, oil and N_2 respectively. At 1500 psi the visible flame (of double base propellants) is relatively close to the burning surface. For more details on double base propellant flame structure see Ref. 3. The most prominent features of the burning under liquid movies is the gas pocket that isolates the burning surface from the surrounding liquid and the pulsating nature of the gas pocket. However, the character of the flame more than 0.5 mm above the surface has only a small influence on the heat feedback to burning surface and, thus, the burning rate.[3] When the propellants were burned under water, a thin layer of propellant at the propellant/water interface did not burn; as shown in Fig. 5, this thin layer acted as a shroud that completely isolated the burning surface from direct contact with the surrounding liquid. When the experiments were conducted under oil, the shroud effect did not occur.

Two differences were noted when the experiment was carried out at 500 psi: (1) the gas bubble above the strand became much larger, and (2) the visible flame occurred in the bubble well above the propellant surface. However, these effects occurred well above the surface and have no appreciable affect on burning rate.

The most important observation in terms of the burning rate determinations is that the burning propellant creates its own gaseous environment that isolates the important reaction zones from the surrounding liquid. It should be noted that at sufficiently low burning rates, the surrounding liquid does interfere with the burning surface. However, HEN-12 burning at 500 psi is well into the domain where the surrounding liquid does not interfere with the burning surface.

Extinguished specimens were recovered for five of the six test conditions. As will be pointed out later, the burning rate in the liquids was nominally 15% lower than in N_2. Figures 6 and 7 show clearly the reason for this. The propellant flame zone adjacent to the liquid is cooled sufficiently that its burning rate at the propellant/liquid interface is lowered. The localized lower burning rate produces the protruding outer edges shown in the cross-section views through specimens I3, I7, I2, and I6 on Figs. 6 and 7. Also, photographs of samples burned in H_2O (I3 and I2) show the film of unburned propellant that remains after the test. Because the strands that are of interest in this study are very thin ($\sim$0.040 inches), the cooling at the propellant/liquid interface affects the burning rate at the midplane of the strand. <u>However, as has been shown in previous studies,[4-6] the burning rates of strands with larger cross-sectional dimensions are not affected by the surrounding liquid</u>.

DATA REDUCTION AND ERROR ANALYSIS

Examination of Observables

First, attention will be given to estimating the errors in the observables: t_b, L, p, Δp, and T_0.

The burning time interval is determined by measuring intervals between the events on the oscillograph and oscilloscope records. First, a scale factor is obtained by measuring the distance ($x_{t,std}$) between a timing interval (t_{std}) which corresponds approximately to the total burning time. Next, the distance (x_t) corresponding to the burning interval is measured. The burning time is obtained as follows:

$$t_b = x_t S_t = x_t (t_{std}/x_{t,std}) \tag{1}$$

Throughout this analysis the estimate of total error will be obtained using the conventional procedure of taking the square root of the sum of the individual errors. Accordingly, the estimate of the error in t_b is*

$$\left[\frac{s_{t_b}}{t_b}\right]^2 \simeq \left[\frac{s_{x_t}}{x_t}\right]^2 + \left[\frac{s_{x_{t,std}}}{x_{t,std}}\right]^2 \tag{2}$$

Since the first and second terms on the left are obtained in a similar manner, to a good approximation

$$s_{t_b} = \sqrt{2}\left[\frac{s_{x_t}}{x_t}\right] t_b \tag{3}$$

The estimate of the errors associated with the length determinations requires more than a knowledge of the length measurement error. Using conventional length measuring devices, surface trimming procedures and jigs for drilling breakwire holes, the distances between the breakwire holes are known to within ±0.003 in. However, the uncertainty in the

*Since the time base provided by the HP226A is extremely accurate, $s_{t_{std}}$ is negligibly small compared to s_{x_t}.

case of breakwire methods is the position of the burning surface with respect to the centerline of the drilled hole ($s_{\Delta L_{breakw}}$) when breakwire burn-out occurs. It is expected that since the identical breakwire placements and configurations determine the start and stop of the timing intervals that the uncertainty of the burning surface location at breakwire burn-out at the start and stop tend to cancel one another. The estimate of error in determining burning interval is

$$\left[\frac{s_L}{L}\right]^2 \simeq \left[\frac{s_{L_{meas}}}{L}\right]^2 + \left[\frac{s_{\Delta L_{breakw}}}{L}\right]^2 \tag{4}$$

Since experience has shown that $s_{L_{meas}}$ is small compared to $s_{\Delta L_{breakw}}$,

$$s_L \simeq s_{\Delta L_{breakw}} \tag{5}$$

For the case of the burning under liquid experiments, the added uncertainty is the degree to which the surface is ignited uniformly ($s_{\Delta L_{ig}}$) or

$$\left[\frac{s_L}{L}\right]^2 \simeq \left[\frac{s_{L_{meas}}}{L}\right]^2 + \left[\frac{s_{\Delta L_{ig}}}{L}\right]^2 \tag{6}$$

The pressure in the chimney burner is calculated by measuring the deflection (y_p) on the oscillograph trace and using it as the point of interpolation in the calibration table, p vs y_p. Since the pressure changes slightly during the tests, a mean pressure is reported

$$\bar{p} = (p_1 + p_2)/2 \tag{7}$$

and the estimate of the $\bar{p}$ error (for the chimney burner) is

$$[s_{\bar{p}}]^2 \simeq [s_{calib}]^2 + [S_p]^2 s_{y_p}^2 \tag{8}$$

Similarly, the estimated error of the pressure increase ($\Delta p = p_2 - p_1$) during the test is

$$s_{\Delta p} = S_p s_{y_p} \tag{9}$$

The pressure in the hydraulic combustor is obtained by summing two components, the set pressure at the beginning of the test (p_{set}) and the mean pressure increase during the test, (Δp). Thus

$$\bar{p} = p_{set} + \overbrace{0.5(y_{p1} + y_{p2})\left(\frac{\Delta p_{std}}{y_{p,std}}\right)}^{\Delta p} \tag{10}$$

where the scale factor S_p is $\Delta p_{std}/y_{p,std}$.

The estimate of the $\bar{p}$ error (in the hydraulic combustor) is

$$[s_{\bar{p}}]^2 \simeq [s_{p,set}]^2 + [S_p]^2 s_y^2 + \Delta p^2 \left[\frac{s_{y_{p,std}}}{y_{p,std}}\right]^2 \tag{11}$$

For the chimney burner tests, the initial temperature is calculated by measuring the deflection on the oscillograph trace and using it as a point of interpolation in the T_0 vs y_T calibration table. Accordingly, the estimate of error is

$$[s_{T_0}]^2 \simeq [s_{calib}]^2 + [S_T]^2 s_{y_T}^2 \tag{12}$$

For the burning under liquid tests, the initial temperature is measured by a mercury in glass thermometer which has ice and boiling point calibrations to within ±0.9 °F.

Calculation of Burning Rate and Errors

Burning rate at the desired pressure, p, and initial temperature, T_0, is obtained by dividing the length of propellant burned, L, by the burning time, t_b, and adjusting the result for the differences between the actual and the intended pressures and initial temperatures (i.e., δr_p and δr_T respectively)*

$$r_{adj} = L/t_b + \delta r_p + \delta r_T \tag{13}$$

Note that the actual burning rate under the prevailing experimental conditions is simply $r = L/t_b$.

To obtain an estimate of the experimental error, each of the terms in Eq. (13) will be analyzed.

To a good approximation (for the propellant and conditions of this study) burning rate behavior can be correlated by the widely used equation

$$r = ap^n \exp[\sigma_p(T_0 - T_{0,ref})] \tag{14}$$

where n and a are nearly constant over a wide region of p and T_0, i.e., ±500 psi at ±30°F. Accordingly, the pressure adjustment, δr_p, can be obtained by considering T_0 constant and differentiating Eq. (14),

$$\frac{dr}{r} = n\frac{dp}{p} \tag{15}$$

Expressed in terms of the pressure differential, $\delta p = p_{intended} - p_{actual}$, the burning rate adjustment

$$\delta r_p = \left(\frac{rn}{p}\right)\delta p \tag{16}$$

Similarly, the adjustment, δr_T, can be obtained by differentiating a logarithmic form of Eq. (14) holding p constant:

*During the subsequent discussion of the multiple breakwire experiments, the determination of burning rate from the slope of the t_b vs x_n regression will be developed and analyzed.

$$\ln r = \ln ap^n + \sigma_p T_0 \tag{17}$$

to obtain

$$\delta r_T = r\sigma_p \delta T_0 \tag{18}$$

where $\delta T_0 = (T_{0,\text{intended}} - t_{0,\text{actual}})$.

As part of this analysis, attention was given to the propagation of errors. For the most part, the errors in the observables (i.e., L, x_t or t_b, p, Δp and T_0) are independent of each other.* This is fortunate. Thus, it is expected that, except in statistically rare situations, the total actual error in burning rate will be algebraically less than the sum of the estimated separate contributions. Accordingly, the conventional procedure of estimating the total error in the experimental method is to take the square root of the sum of the squares of the individual errors. This method has the compensating properties required for combining the individual contributions to the total error in the experimental method. Accordingly, the error in the method of determining burning rate is

$$[s_r]^2 \simeq \left[\frac{\partial r}{\partial L}\right]^2 s_L^2 + \left[\frac{\partial r}{\partial t_b}\right] s_{t_b}^2 + s_{\delta r_p}^2 + s_{\delta r_T}^2 \tag{19}$$

where the partial differentiation of Eq. (13) yields

$$\frac{\partial r}{\partial L} = \frac{r}{L}$$

and

$$\frac{\partial r}{\partial t_b} = -\frac{r}{t_b} \tag{20}$$

Dividing through by r^2 and rearranging terms in Eq. (19),

$$\left[\frac{s_r}{r}\right]^2 \simeq \left[\frac{s_L}{L}\right]^2 + \left[\frac{s_{t_b}}{t_b}\right]^2 + \left[\frac{s_{\delta r_p}}{r}\right]^2 + \left[\frac{s_{\delta r_T}}{r}\right]^2 \tag{21}$$

---

*This is a reasonable notion since the individual values associated with each observable are measured using different instruments.

Using Eqs. (16) and (18) to approximate the error in evaluating $s_{\delta r_p}$ and $s_{\delta r_T}$ yields

$$\left[\frac{s_{\delta r_p}}{r}\right]^2 \simeq \left(\frac{\delta r_p}{r}\right)^2 \left[\left(\frac{s_r}{r}\right)^2 + \left(\frac{s_n}{n}\right)^2 + \left(\frac{s_{\delta_{p/p}}}{\delta_{p/p}}\right)^2\right] \tag{22}$$

and

$$\left[\frac{s_{\delta r_T}}{r}\right]^2 \simeq \left(\frac{\delta r_T}{r}\right)^2 \left[\left(\frac{s_r}{r}\right)^2 + \left(\frac{s_{\sigma_p}}{\sigma_p}\right)^2 + \left(\frac{s_{\delta T_0}}{\delta T_0}\right)^2\right] \tag{23}$$

Finally, the estimate of the burning rate error is obtained by using Eqs. (4), (3), (16), (18), (22), and (23) to evaluate the component terms in Eq. (21).

Burning Rate Data From Chimney Burner

Burning rate data were obtained in the chimney burner over the following range of conditions:

Pressure, psia	515, 1015 & 1515
Temperature, °F	20, 80, & 140
N_2 Flow	low, high and none

The tests and data reduction were carried out using the methods described in the previous sections. Table I summarizes the reduced and raw data for the entire test series. Table II contains the times of breakwire burn-out. The spacing between the centers (obtained using an optical comparator) of the breakwire holes for five of the strands is given in Table III. The standard deviation of the hole spacing is less than 0.002 in. and the range of the measurements for an individual breakwire interval is less than 0.003 in. Based on examining the consistency of the burning rate data over each one-half inch interval (see Table IV), an estimate of 0.010 in. for $s_{\Delta L,breakw}$ was used*.

The equations developed for estimating errors were applied at the lowest pressure and the highest pressure (i.e., typically the conditions for specimens N10 and N12 respectively). First, the errors associated with the observables were evaluated (see Table V). Next, knowledge about the errors in the observables was used to evaluate Eq. (21) which provides an estimate of the overall error (see Table VI). While Tables V and VI are largely self-explanatory, several items were worthy of note. The error contributions of δr_p and δr_T can be made negligible by refining the experiment so that p and T_0 are within 5 psi and 2 °F, respectively, of the desired values. Also on the second iteration of the data, the values of s_r, s_n, and s_{σ_p} can be reduced greatly. The error associated with time measurement is acceptable. Thus, in terms of production considerations where everything is well controlled, the

*The appropriateness of this estimate can be seen by examining the averaged deviation at the bottom of Table IV in terms of Eq. 21 for L≃0.5 in.

major contributor to burning rate uncertainty is s_L. As shown in the next section, the most direct method of eliminating the detrimental effect of the rather large s_L is to increase the strand length so as to reduce s_L/L. Since the errors associated with δr_p and δr_T can be made arbitrarily small by improving the pressure and temperature control and since s_{t_b} is already very small, under production conditions it is expected that the standard error of this burning rate determining method can be held to within 0.5%. Several of the points were replicated to test the precision of the experimental method. Specimens 11, 12 & 13 were tested at nearly identical conditions and produced burning rates within 0.8% of the mean. However, specimens 22 and 24 were within 2.5% of each other. Possibly, this is an indication of experimental difficulties at the lower T_0 conditions.

Multi-Breakwire Data Reduction. The time and distance intervals from the multi-breakwire experiments can be used to obtain an estimate of dx/dt from the linear regression line

$$\hat{t} = a_0 + a_1 x \tag{24}$$

since

$$dx/dt = a_1^{-1} \tag{25}$$

In terms of the 7 t_n and x_n pairs

$$dx/dt = \left[\frac{\Sigma t_n x_n - \frac{\Sigma x_n \Sigma t_n}{n}}{\Sigma x_n^2 - \frac{\Sigma x_n^2}{n}} \right]^{-1} \tag{26}$$

The degree to which the t_n and x_n pairs lie on a straight line is a measure of the consistency of the data. The least squares linear regressions through 4 sets of points are shown on Fig. 8. Note that in all cases the fit is good. However,

specimen 6 has error about twice as large as the others. As seen from Table I in most cases the coefficient of variation in the burning determined in this manner is less than 0.5% or about the same as the standard error predicted by the error analysis. Another indication of the consistency of the data is obtained by comparing burning rates obtained by using Eq. (13) and $L = x_7 - x_0$ with rates obtained from the linear regression (see the second to last column in Table I). Note that with exception of specimen 3 & 11 burning rates obtained by the two methods are within 0.5% of each other. Thus, when the data are consistent either method is satisfactory. However, when the data are inconsistent, the linear regression method quickly identifies the suspect t_n, r_n pairs. Also, if the final or initial breakwire data point is lost for some reason, the remaining t_n, r_n pairs are usually adequate for the burning rate determination.

Effect of Strand Length on Error

The percentage errors in length and time measurements are less for long strands than for short strands. The advantages of longer strands can be evaluated using the first two terms of Eq. (21)* to consider how the error decreases as length of the timed interval is increased. Thus the following time and distance intervals (available in the multi-breakwire experiment) were considered for breakwire pairs distance L apart:

No. of Intervals	Distance, L	Time, t_b
1	$d_2 - d_1$	$t_2 - t_1$
2	$d_3 - d_1$	$t_3 - t_1$
3	$d_4 - d_1$	$t_4 - t_1$
4	$d_5 - d_1$	$t_5 - t_1$
5	$d_6 - d_1$	$t_6 - t_1$
6	$d_7 - d_1$	$t_7 - t_1$

and it was assumed that the absolute magnitude of the time and distance errors were not affected by strand length, i.e., the oscillograph speed was not changed.

In terms of the previous development, the estimate of the error as a function of $L = nd$ is

$$\frac{s_r}{r} = \left\{ \left[\frac{s_L}{nd}\right]^2 + \left[\frac{s_{t_b}}{n\Delta t}\right]^2 \right\}^{1/2}$$

$$= \left\{ \left[\frac{s_L}{nd}\right]^2 + 2\left[\frac{s_{x_t}}{nx_t}\right]^2 \right\}^{1/2} \qquad (27)$$

$$= \left\{ \left[\frac{0.005}{n0.5}\right]^2 + 2\left[\frac{0.01}{n9.0}\right]^2 \right\}^{1/2}$$

Eq. (24) evaluated for distances from 0.5 to 3.0 inches is shown in Table VII.

---

*Using only the first two terms of Eq. (21) implies that the experimental procedure is refined to the point that the errors associated with δ_p and δT_0 are negligibly small.

Burning Rate Data from Burning Under Liquid Combustor

Burning rate data were obtained over the following range of conditions:

Pressure, psia	510 & 1515
Temperatures, °F	80 & 140
Liquids	H_2O and oil

The tests and data reduction were carried out using the methods described in the previous sections. Tables VIII and IX summarize the reduced data from the entire test series. Table X is a set of sample calculations that illustrate the data method.

The test-to-test variability for the burning under water experiments was quite small (i.e., the coefficient of variation is 0.8% or less). On the other hand, the test-to-test variability of the burning under oil experiments was large and generally unsatisfactory. Furthermore, the burning rate at 1515 psia and 140 °F were anomalously (but consistently) high indicating that the oil vapors may have been augmenting the flame zone reactions.

For the very thin strands (which were of particular interest in this study), the burning media has a profound influence on burning rate. Indeed, as shown in Fig. 9, the burning rates under liquid were nominally 15% less than those in nonflowing N_2.

The origin of the lower burning rates in H_2O and oil is obvious from examining the photographs in Figs. 4, 5, and 6, i.e., heat loss at the propellant/liquid interface significantly lowers the burning rate. Since the strands that are of interest in this study are very thin (0.04 inches), the thin layer affected by the interface cooling is a large fraction of the total thickness of the strand and, as a consequence, the center portion of the strand has a reduced burning rate. If a thicker strand were used (e.g., 0.2 inches), the cooling of the outer layer would not affect the burning rate at the center of the strand and the center region of the strand would regress with a flat surface.

The lower burning rates coupled with the difficulties encountered with burning under oil make it apparent that burning under liquid is not appropriate for HEN-12 sheet propellant. The lower burning rate under liquid is consistent with the lower burning rate at edges of extinguished specimens (recall Figs. 6 and 7).

The choice of oil was constrained by the nature of these experiments. We needed a clear oil for the photographic studies, a high flash point oil so that oil vapors would not combust in the flame zone, an oil that would remain fluid at low temperatures (e.g., 0 °F), and an inexpensive oil which can be used in production testing. Of the foregoing needs, we achieved only the first. As previously stated, the oil vapors apparently caused serious problems at 140 °F. We were unable to conduct successfully experiments in the 0 to 20 °F range because once the oil became slightly contaminated it would thicken to the point that pressure transmission to the transducers was erratic. However, because of the general reduction in burning rate in liquids there was no reason to try to overcome the problems by experimenting with more suitable oils.

It is emphasized that the reduction in burning rate experienced in this test series is a direct consequence of the unusually thin strands which are of interest in the study. Previous[4,5,6] studies have demonstrated that when a sufficiently thick strand is used the burning rates in liquids are within a few percent of the burning rates in N_2.

DISCUSSION OF BURNING RATE DATA

The burning rate points were adjusted to the desired pressure and temperatures using the δr_p and δr_T correction and plotted on the conventional coordinate system (i.e., ln r vs ln p and ln r vs T_0). Unless indicated otherwise the lines and slopes (i.e., n and σ_p) on Figs. 9 through 13 are from least squares linear regressions.

Effect of Media on Burning Rate

Figure 9 illustrates clearly the large effect that the media surrounding the strand has on burning rate. Naturally, the condition that least affects burning rate is the nonflowing N_2. The results of Table I and Fig. 9 show that uninhibited strands can burn in a uniform and reproducible manner and that N_2 flow is not needed to eliminate flame spreading along the side of the strand. From these results, it was concluded that the N_2 flow was not needed, strand inhibition was not required, and burning under liquid produced a large (15%) reduction in burning rate.

Figure 10 is included to emphasize the unusual burning rates produced by burning under oil at 140 °F. At 510 psi, three of the data points for burning under oil are 30% higher than the corresponding data for burning under H_2O. Also at the higher pressure, the data variation is much greater when oil is used. Figure 11 is included for completeness to show the 25% variation in σ_p between the 510 and 1515 psi conditions when liquids are used. The σ_p variation in the nonflowing N_2 test was approximately 5%.

Accordingly, once the inconsistency of the burning under liquid results were interpreted, the original test plan was modified so that greater emphasis could be placed on obtaining data in nonflowing N_2.

Burning Rate Data Obtained Under Preferred Conditions

Figures 12 and 13 show the degree of the consistency of the data obtained in nonflowing N_2 over the range of test conditions. With the exception of two data points (Specimens

11 and 22) the data correlation [using Eq. (14)] are very good. The coefficient of determination of the regression lines on Figs. 12 and 13 are 0.999 or better except for the $r(T_0)$ line at 1015 psi which is 0.997.

It should be noted that the scope of this study did not include sufficient tests in nonflowing N_2 for a proper statistical determination of strand-to-strand repeatability.

CONCLUSIONS

The results of this study in terms of the objectives and questions described in the introduction are conclusive. The HEN-12 sheet propellant can be burned uniformly and reproducibly in nonflowing N_2 and inhibition is not required to prevent flame spreading down the side of the strand. Burning under liquids or in flowing N_2 provides no improvements. For the particular production control application which prompted this study, no significant improvement in the quality of the data is obtained by using multiple breakwire instrumentation that justifies the added complications associated with the 5 additional breakwires. [Multiple breakwire instrumentation is of great value when information is sought on propellants with nonuniform burning properties.]

In the 500 to 1500 psi and 20 to 140 °F range, the HEN-12 propellant demonstrated very consistent and uniform burning rate characteristics. Analysis of the various sources of errors indicates that the experimental method has an error of less than 0.5%. The regression analysis of the multiple breakwire data repeatedly produced burning rate coefficient of variations of less than 0.5%.

NOTE: The readers of this report are asked to keep in mind that the large variations in burning rate in H_2O and N_2 are a direct result of the abnormally thin strands which were of special interest in this study. The burning media does not influence burning rate when strands of normal dimensions are burned at sufficiently high pressure. It is hoped that this report does not convey the impression that burning in liquid reduces the burning rate of conventional strands.

REFERENCES

1. "Standard Methods and Procedures for the Strand Burning Rate Evaluation of Rocket Propellant Powder," U.S. Navy Bureau of Ordnance, NAVORD OD9376, 29 May 1953.

2. Steinz, J. A., Stang, P. L., and Summerfield, M., "The Burning Mechanism of Ammonium Perchlorate-Based Composite Solid Propellants," AIAA Paper 68-658, June 1968; also AMS Report No. 830, February 1969, Princeton University, Princeton, N.J.

3. Kubota, N., Ohlemiller, T. J., Caveny, L. H., and Summerfield, M., "The Mechanism of Super-Rate Burning of Catalyzed Double Base Propellants," Report No. AMS 1087, Department of Aerospace and Mechanical Sciences, Princeton University, Princeton, N.J., March 1973. (AD 763-786)

4. Cole, R. B., "Burning Rates of Solid Composite Propellants at Pressures up to 20,000 psig (U)," Report No. S-80, September 15, 1966, Rohm and Haas, Huntsville, Alabama.

5. Koury, J. L., "Solid Strand Burn Rate Technique for Predicting Fullscale Motor Performance," Air Force Rocket Propulsion Laboratory, Report AFRPL-TR-73-49, October, 1973.

6. Saber, A. J., Johnston, M.D., Caveny, L. H., Summerfield, M., and Koury, J. L., "Acoustic Emissions from Burning Propellant Strands," Proceedings of the 11th JANNAF Combustion Conference, Dec. 1974, CPIA Publication No. 261, Vol. I, pp. 409-427.

TABLE

CHIMNEY BURNER REDUC

INTENDED, P, PSIG	INTENDED, T_0, °F	SPECIMEN NO. SB-	PRESS. DEFLECT INITIAL, $y_{p,1}$, IN	PRESS. DEFLECT FINAL, $y_{p,2}$, IN	TEMP. DEFLECT. y_T, IN	TIMESCALE FACTOR, SEC/CM	$x_{t,1}$, CM	$x_{t,2}$	$x_{t,3}$	$x_{t,4}$	$x_{t,5}$	
500.	80.	L 3	2.18	2.16	1.16	0.1268	0.00	4.92	9.94	14.87	19.62	2
1000.	80.	L 4	4.06	4.06	1.12	0.0626	0.00	7.31	14.68	22.18	29.18	3
1500.	80.	L 5	5.75	5.75	1.18	0.0634	0.00	5.95	12.14	18.27	24.12	3
500.	80.	H 8	2.18	2.18	1.10	0.0634	0.00	10.10	20.16	30.67	39.78	4
1000.	80.	H 7	4.10	4.10	1.09	0.0634	0.00	7.53	15.04	22.54	29.55	3
1500.	80.	H 6	5.77	5.77	1.10	0.0634	0.00	6.37	0.00	20.02	25.79	3
500.	80.	N10	2.18	2.28	1.25	0.0633	0.00	9.62	18.70	28.86	37.76	4
1000.	80.	N14	4.10	4.23	1.29	0.0635	0.00	6.95	13.88	21.10	27.78	3
1500.	80.	N11	5.76	5.90	1.40	0.0635	0.00	8.08	13.72	19.46	24.65	3
1500.	80.	N12	5.76	5.90	1.31	0.0635	0.00	6.04	11.98	17.74	23.16	2
1500.	80.	N13	5.77	5.90	1.32	0.0634	0.00	5.70	11.75	17.47	22.80	2
500.	140.	N17	2.18	2.25	2.33	0.0633	0.00	8.98	17.41	26.35	34.82	4
1000.	140.	N16	4.11	4.23	2.13	0.0633	0.00	6.25	0.00	19.05	24.97	3
1500.	140.	N15	5.77	5.91	2.19	0.0633	0.00	0.00	0.00	0.00	20.48	2
500.	20.	N26	2.11	2.11	-0.23	0.0639	0.00	11.64	22.63	34.21	45.20	5
1000.	20.	N22	4.12	4.10	-0.29	0.0632	0.00	8.40	15.90	0.00	32.49	4
1000.	20.	N25	4.14	4.12	-0.33	0.0638	0.00	8.36	16.51	25.03	33.10	4
1500.	20.	N24	5.80	5.80	-0.36	0.0638	0.00	7.13	13.58	20.34	26.78	3

*L-low N_2 flow, H-high N_2 flow, & N-no N_2 flow.

NOTES: Propellant XM36(PE463-3 sub-lot #2 Sheet 24).
Nominal strand dimensions 0.18 x 0.040 x 4.2 inches.

TABLE I

URNER REDUCED AND RAW DATA

$x_{t,4}$	$x_{t,5}$	$x_{t,6}$	$x_{t,7}$	ACTUAL, $\bar{P}$, PSIG	ACTUAL, T_0', °F	r_{adj} IN/SEC	COEF. OF VARIATION (S_r/r) x 100%	COEFFICIENT OF DETERMINATION	$r_{adj}/r_{0-7,adj}$	PRESS. RISE DURING TEST
.87	19.62	24.71	29.24	495.	83.	0.781	0.44	0.99993	1.001	-5.
.18	29.18	36.52	44.02	1006.	81.	1.063	0.14	0.99999	0.999	0.
.27	24.12	30.06	36.05	1540.	84.	1.258	0.36	0.99993	0.996	0.
.67	39.78	49.96	60.27	497.	81.	0.774	0.33	0.99994	1.001	0.
.54	29.55	36.78	44.28	1018.	80.	1.043	0.30	0.99995	1.000	0.
.02	25.79	31.97	38.30	1546.	81.	1.191	1.01	0.99959	0.995	0.
.86	37.78	47.25	56.79	510.	87.	0.798	0.30	0.99995	0.998	24.
.10	27.78	34.40	41.24	1038.	89.	1.079	0.47	0.99989	0.996	40.
.46	24.65	30.00	36.00	1566.	93.	1.316	0.64	0.99983	1.007	47.
74	23.16	28.57	34.23	1566.	90.	1.300	0.83	0.99966	1.002	47.
47	22.80	28.60	34.10	1568.	90.	1.298	0.63	0.99980	0.997	44.
35	34.82	43.27	51.96	506.	133.	0.907	0.24	0.99997	0.999	17.
05	24.97	31.24	37.48	1040.	124.	1.265	0.31	0.99996	0.997	37.
00	20.48	25.67	30.85	1570.	127.	1.526	0.11	1.00000	0.999	47.
21	45.20	53.12	0.00	481.	21.	0.691	0.23	0.99999	1.002	0.
00	32.49	40.75	48.92	1021.	19.	0.946	0.51	0.99990	0.998	-6.
03	33.10	41.47	49.77	1027.	17.	0.922	0.17	0.99999	0.997	-6.
34	26.78	33.64	40.32	1556.	15.	1.143	0.32	0.99995	1.002	0.

TABLE II
TIMES OF BREAKWIRE BURN-THROUGH
FROM CHIMNEY BURNER TEST

SPEC. NO.	t_0, sec	t_2	t_3	t_4	t_5	t_6	t_7
L 3	0.000	0.624	1.260	1.886	2.488	3.133	
L 4	0.000	0.458	0.919	1.388	1.827	2.286	2.756
L 5	0.000	0.377	0.770	1.158	1.529	1.906	2.285
H 8	0.000	0.640	1.278	1.944	2.522	3.167	3.821
H 7	0.000	0.477	0.953	1.429	1.873	2.331	2.807
H 6	0.000	0.404		1.269	1.635	2.027	2.428
N10	0.000	0.609	1.183	1.826	2.389	2.990	3.593
N14	0.000	0.441	0.881	1.340	1.764	2.184	2.618
N11		0.513	0.872	1.237	1.567	1.906	2.288
N12	0.000	0.383	0.761	1.126	1.470	1.814	2.173
N13	0.000	0.361	0.745	1.108	1.446	1.814	2.162
N17	0.000	0.568	1.102	1.668	2.204	2.739	3.289
N16	0.000	0.396		1.206	1.581	1.978	2.374
N15	0.000				1.297	1.626	1.954
N26	0.000	0.744	1.446	2.186	2.888		
N22	0.000	0.531	1.005		2.053	2.575	3.091
N25	0.000	0.533	1.053	1.597	2.112	2.646	3.175
N24	0.000	0.455	0.866	1.297	1.708	2.146	2.572

Note: Blanks in the table indicate data points which were lost because time of breakwire burn through was not clearly distinguishable.

Table III

Measurements of Breakwire Position (Chimney Burner)

SPECIMEN SB	x_1	x_2-x_1	x_3-x_2	x_4-x_3	x_5-x_4	x_6-x_5
1	0.5020	0.4843	0.5033	0.4697	0.4896	0.5022
6	0.5013	0.4840	0.5038	0.4714	0.4902	0.5020
11	0.5017	0.4838	0.5032	0.4732	0.4900	0.5010
16	0.5015	0.4836	0.5028	0.4742	0.4894	0.5005
22	0.5009	0.4821	0.5046	0.4722	0.4908	0.5008
$\overline{\Delta x}$	0.5015	0.4836	0.5035	0.4721	0.4900	0.5013
s_x	0.0004	0.0008	0.0007	0.0017	0.0005	0.0008
Range	0.0006	0.0015	0.0011	0.0024	0.0008	0.0009
$\Sigma\overline{\Delta x}$	0.5015	0.9851	1.4886	1.9607	2.4507	2.9520

Holes drilled with No. 76 bit (0.020 in).
Lengths are in inches.

Table IV

COMPARISON OF BURNING RATES MEASURED OVER EACH OF THE BREAKWIRE INTERVALS (CHIMNEY BURNER)

I.E., L ≃ 0.5 INCHES

INTENDED, P, PSIG	INTENDED, T_0, °F	SPECIMEN NO. SB-	εr_1 %	εr_2 %	εr_3 %	εr_4 %	εr_5 %	εr_6 %	$r_{adj}/r_{0-7,adj}$
500.	80.	L 3	2.7	-3.0	2.9	0.1	-3.1		1.0012
1000.	80.	L 4	2.4	-2.0	0.3	0.7	-0.4	-0.1	0.9988
1500.	80.	L 5	3.3	-4.2	0.7	-1.0	1.0	2.7	0.9959
500.	80.	H 8	1.3	-1.9	-2.2	5.8	-1.9	-0.7	1.0005
1000.	80.	H 7	-0.2	-3.5	0.7	1.0	1.5	0.3	1.0004
1500.	80.	H 6	2.6		-5.7	6.7	3.2	3.4	0.9953
500.	80.	N10	0.5	2.7	-4.4	2.3	-0.6	1.4	0.9978
1000.	80.	N14	1.2	-2.2	-2.2	-0.9	3.7	2.9	0.9963
1500.	80.	N11		-3.0	-0.8	2.9	3.5	-5.4	1.0073
1500.	80.	N12	-3.9	-5.8	1.2	0.8	4.7	2.7	1.0016
1500.	80.	N13	2.0	-7.4	2.1	2.7	-2.2	5.8	0.9965
500.	140.	N17	-1.6	1.0	-0.8	-1.8	2.0	1.8	0.9991
1000.	140.	N16	2.2		-1.8	1.6	-0.6	2.5	0.9968
1500.	140.	N15				0.1	-1.4	1.3	0.9993
500.	20.	N26	-0.9	1.3	0.1	-1.1			1.0017
1000.	20.	N22	-0.8	7.1		-2.3	-1.6	2.0	0.9977
1000.	20.	N25	1.4	0.3	-0.1	-1.1	-1.1	2.2	0.9972
1500.	20.	N24	-4.1	2.2	1.6	-0.0	-2.7	2.4	1.0018
		$\Sigma\varepsilon r$ =	8.0	-18.3	-8.4	16.3	4.0	25.4	
		$[\Sigma\varepsilon r^2/n]^{0.5}$ =	2.3	3.8	2.2	2.5	2.4	2.8	

$$\Sigma(r_{adj}/r_{0-7,adj} - 1) = -0.0148$$

$$[\Sigma(r_{adj}/r_{0-7,adj} - 1)^2]^{0.5} = 0.0030$$

*εr's are differences between burning rate over a particular interval and the mean burning rate obtained from the linear regression.

Table V

Estimation of Errors in Observables from Chimney Burner Experiments

(Values are typical for first iteration.)

	EQUATION	PRESSURE, PSI		COMMENTS
		500	1500	
OBSERVABLES:				
Lengths burned:	(5)			
d, in		0.5	→	
s_d, in		0.01	→	Inherent in system
s_d/d		0.020	→	
L, in		3	→	
$s_L = s_d$, in		0.01	→	Inherent in system
s_L/L		0.0033	→	
t_b to burn distance d:	(3)			
t_b, sec	(1)	0.60	0.35	
x_t, cm		10	6	
s_{x_t}, cm		0.01	→	†
s_{t_b}, sec		0.0009	0.0009	
t_b to burn distance L:	(3)			
t_b, sec	(1)	3.5	2.2	
x_t, cm		58	34	
s_{x_t}, cm		0.01	0.01	†
s_{t_b}, sec		0.0009	0.0009	
Pressure:	(8)			
s_{calib}, psi		2.5	→	
S_p, psi/in		250	→	
s_y, in		0.01	→	†
$S_p s_y$, psi		2.5	→	
s_p, y psi		3.5	→	
s_p/p		0.007	0.002	
Difference between p_{actual} & $p_{desired}$:	(9)			
δp, psi		20	50	
$s_{\delta p}$, psi		2.5	→	†
$s_{\delta p}/\delta p$		0.13	0.05	
Initial Temperature:	(12)			
s_{calib}, °F		1	→	
S_r, °F/in		50	→	
s_y, in		0.1	→	
s_{T_0}, °F		1.1	→	

*All values are rounded off to represent approximate range of the variable for the purpose of the error analysis.

†Measurement accuracy.

Table VI **Estimation of Burning Rate Measurement Errors Using Eq. 21 for Chimney Burner**

TERM IN EQ.21	EQUATION OR TABLE	COMPONENT ERRORS		OVERALL TERM		COMMENTS
		PRESSURE		PRESSURE		
		500	1500	500	1500	
$\left[\frac{s_L}{L}\right]$ =				0.0034	0.0034	
s_L	(5)	0.01	→			Inherent error.
L		3.0	→			
$\left[\frac{s_{t_b}}{t_b}\right]$ =				0.0002	0.0003	
s_{t_b}	(3)	0.0009	0.0009			Error is no problem.
t_b	V	3.8	2.3			
$\left[\frac{s_{\delta r_p}}{r}\right]$ =	(22)			0.0033	0.0018	
δr_p	(16)	0.0156	0.019			
r	-	0.8	1.3			
$\delta r_p / r$	-	0.0195	0.0146			
s_r / r	*	0.05	→			Can be reduced to 0.01 on second iteration
s_n / n	*	0.1	→			Can be reduced to 0.02 on second iteration.
$s_{\delta p} / \delta p$	V	0.13	0.05			Big contributor to error if δp is large
$\left[\frac{s_{\delta r_T}}{r}\right]$ =	(23)			0.0033	0.0033	
δr_T	(18)	0.014	0.022			
$\delta r_T / r$	-	0.017	0.017			
s_r / r	*	0.05	→			Can be reduced to 0.01 on next iteration.
s_{σ_p} / σ_p	*	0.1	→			Can be reduced to 0.05 on next iteration.
$s_{\delta T_0}$	V	1.1	→			
$s_{\delta T_0} / \delta T_0$	-	0.15	→			
			$\frac{s_r}{r}$ =	0.0057	0.0051	

*Value selected as reasonable guideline. However, considerable improvements are obtainable once $r(p,T_0)$ data are known.

Table VII

Effect of Length Burned on Error (Chimney Burner)

[Evaluated by means of Eq. (21)]

n	Length Burned in.	$\frac{s_L}{nd}$	$\frac{s_{x_t}}{nx_t}$	$\frac{s_r}{r} \times 100$ %
1	0.5	0.0200	0.00111	2.0
2	1.0	0.0100	0.00056	1.0
3	1.5	0.0067	0.00037	0.7
4	2.0	0.0050	0.00028	0.5
5	2.5	0.0040	0.00022	0.4
6	3.0	0.0033	0.00019	0.3

Assume that $d = 0.5$ in and that $s_L = 0.01$.

TABLE VIII

REDUCED DATA FROM BURNING UNDER WATER EXPERIMENTS

TEST NO.	P_{des} PSIA	$T_{0,des}$ °F	δp† PSI	$\delta r_p = \frac{\partial r}{\partial p}\delta p$ IN/SEC	δT_0‡ °F	$\delta r_T = \frac{\partial r}{\partial T_0}\delta T_0$ IN/SEC	r IN/SEC	r_{adj} IN/SEC	$C_{v,r}$ %
IP-54	510	80	-20	-0.011	+10.8	+0.013	0.666	0.668	
55			-20	-0.011	+10.8	+0.013	0.670	0.672	
56			-23	-0.013	+10.8	+0.013	0.659	0.659	
57			-22	-0.012	+10.8	+0.013	0.661	0.662	
58			-18	-0.011	+10.8	+0.013	0.660	0.662	
							$\bar{r}$ =	0.665	0.8%
							$C_{v,\bar{r}}$ =	0.4%	
59	510	140	-32	-0.020	-0.9	-0.001	0.760	0.739	
61			-32	-0.020	-2.2	-0.002	0.755	0.733	
62			-24	-0.015	-2.0	-0.002	0.755	0.738	
63			-23	-0.015	-2.0	-0.002	0.757	0.740	
							$\bar{r}$ =	0.738	0.4%
							$C_{v,\bar{r}}$ =	0.2%	
66	1515	140	-40	-0.015	+2.5	+0.007	1.239	1.231	
67			-30	-0.011	+2.5	+0.007	1.243	1.239	
68			-26	-0.010	+2.5	+0.007	1.243	1.240	
							$\bar{r}$ =	1.237	0.4%
69	1515	80	-20	-0.006	+8.0	+0.018	1.055	1.067	
70			-4	-0.001	+8.0	+0.018	1.058	1.075	
71			0	0	+8.0	+0.018	1.053	1.071	
							$\bar{r}$ =	1.071	0.4%

† Difference between $p_{desired}$ and p_{actual}.

‡ Difference between $T_{0,desired}$ and $T_{0,actual}$.

TABLE IX

REDUCED DATA FROM BURNING UNDER OIL EXPERIMENTS[+]

TEST NO.	p_{des} PSIA	$T_{0,des}$ °F	δp † PSI	$\delta r_p = \frac{\partial r}{\partial p}\delta p$ IN/SEC	δT_0 ‡ °F	$\delta r_T = \frac{\partial r}{\partial T_0}\delta T_0$ IN/SEC	r IN/SEC	r_{adj} IN/SEC	$C_{v,r}$ %
IP-72	510	80	-26	-0.014	+12.0	+0.014	0.689	0.689	
73			-34	-0.019	+11.8	+0.014	0.720	0.715	
74			-33	-0.018	+11.6	+0.014	0.684	0.680	
75			-32	-0.018	+11.3	+0.013	0.698	0.693	
							$\bar{r}$ =	0.694	2.1
76	1515	80	-44	-0.013	+10.4	+0.024	1.066	1.077	
77			-45	-0.014	+10.2	+0.023	1.069	1.078	
78			-39	-0.012	+10.2	+0.023	1.066	1.077	
							$\bar{r}$ =	1.077	0.1
79	1515	140	-53	-0.020	0	0	1.206	1.186	
80			-35	-0.013	0	0	1.261	1.248	
81			-33	-0.012	+0.4	+0.000	1.237	1.250	
82			-25	-0.009	+0.4	+0.000	1.225	1.216	
							$\bar{r}$ =	1.225	2.5
83	510	140	-37	-0.024	+0.5	+0.001	1.102	1.079	
84			-40	-0.026	+0.5	+0.001	0.894	0.869	
85			-37	-0.024	+0.7	+0.001	1.075	1.052	
86			-33	-0.021	+0.7	+0.001	1.093	1.073	
							$\bar{r}$ =	1.018	9.8

+Crisco cooking oil was used.

†Difference between $p_{desired}$ and p_{actual}.

‡Difference between $T_{0,desired}$ and $T_{0,actual}$.

Table X

Sample Calculation

Data Reduction for Burning Under Liquid Experiments

Test IP 54 $p_{desired} = 510$ psia, $T_{0,desired} = 80$ °F

$$\Delta\bar{p} = \Delta\bar{p}_{std} \frac{y_{p1} + y_{p2}}{2y_{p,std}} = 50.0 \frac{0.50 + 0.40}{2 \times 1.10} = 20 \text{ psi}$$

$$\bar{p}_{actual} = p_{set} + \Delta\bar{p} + p_{error} + 14.7 \simeq 500 + 20 - 5 + 14 = 530 \text{ psia}$$

$$t_b = t_{std} \frac{x_t}{x_{t,std}} = 3.000 \frac{5.79}{5.79} = 3.00 \text{ sec}$$

$$r = \frac{L}{t_b} = \frac{2.000}{3.00} = 0.666 \text{ in/sec}$$

$$\delta p = p_{desired} - \bar{p}_{actual} = 510 - 530 = -20 \text{ psi}$$

$$\delta r_p = r_{adj} \frac{n_{adj}}{p} \delta p = - 0.665 \frac{0.435}{530} 20 = -0.011 \text{ in/sec}$$

$T_{0,actual} = 69.2$ °F

$$\delta T_0 = T_{0,desired} - T_{0,actual} = 80.0 - 69.2 = 10.8 \text{°F}$$

$$\delta r_T = r\sigma_p \delta T_0 = 0.666 \times 0.0018 \times 10.8 = 0.013 \text{ in/sec}$$

$$r_{adj} = r + \delta r_p + \delta r_T = 0.666 - 0.011 + 0.013 = 0.668 \text{ in/sec}$$

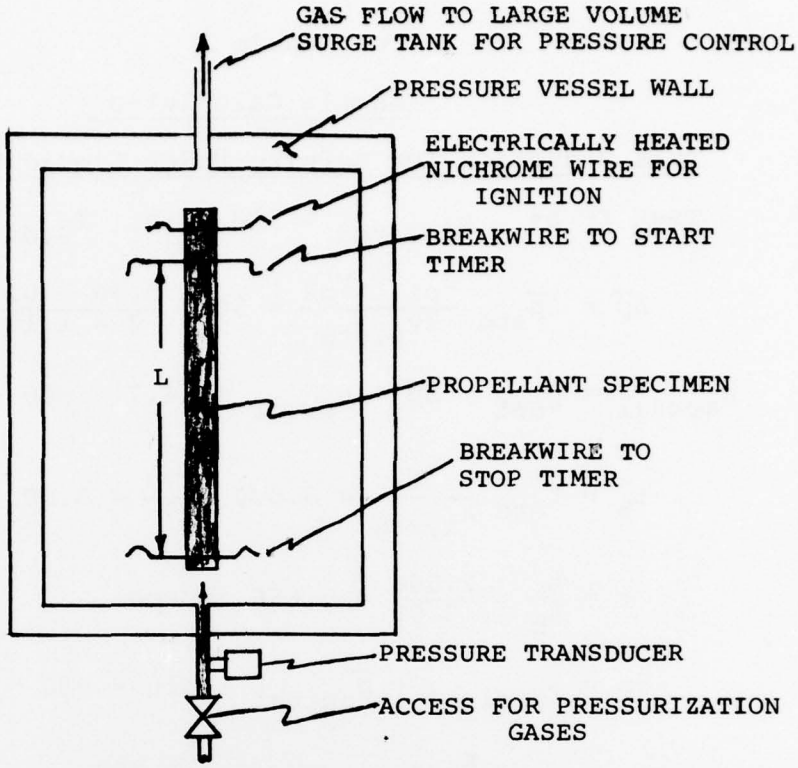

a) Single burning interval strand burner.

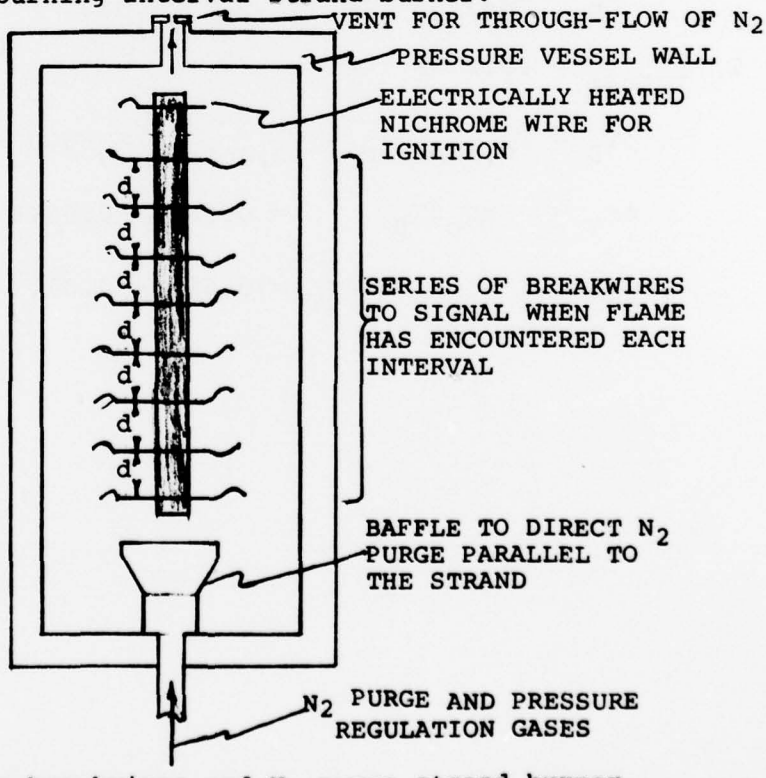

b) Multiple breakwires and N_2 purge strand burner.

Fig. 1 Strand burners for determining propellant burning rates in N_2.

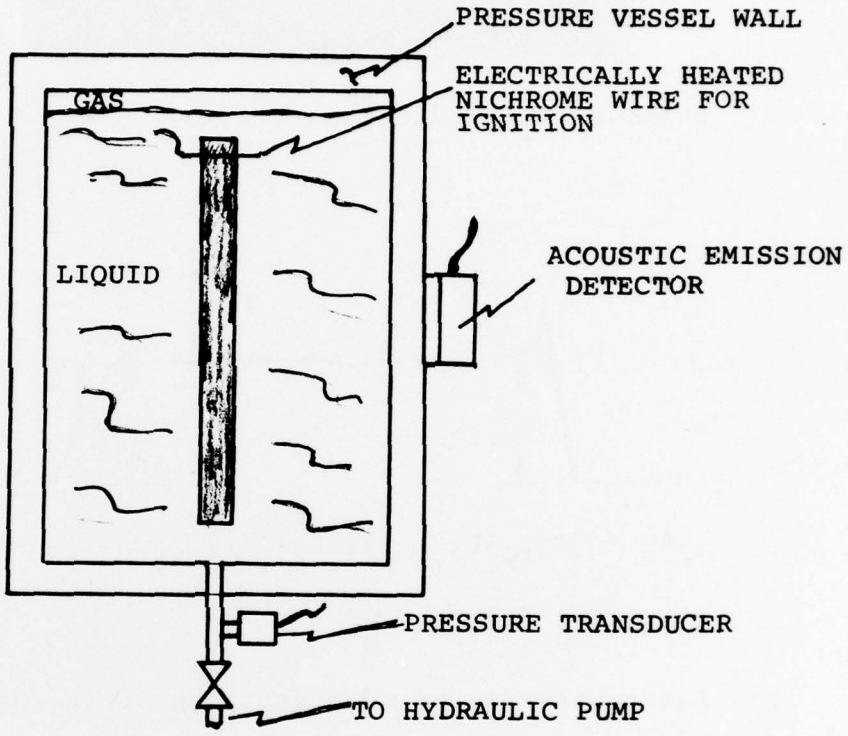

Fig. 2 Strand burner for determining propellant burning rates under liquid.

Note: At sufficiently high burning rates, burning surface does not come into contact with liquid since combustion products form local gaseous environment (i.e., a bubble) around the end of the strand.

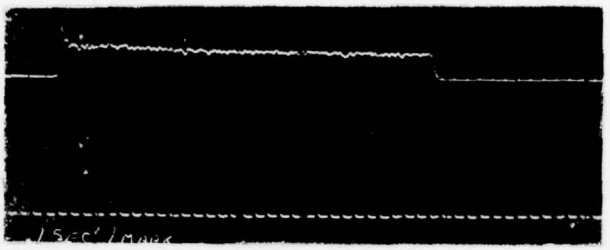

a) Example of oscilloscope record

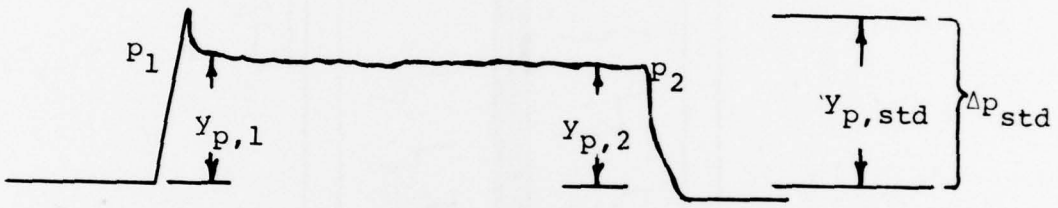

$$\Delta p = \Delta p_{std}(y_{p,1} + y_{p,2})/(2y_{p,std})$$

$$\bar{p}_{actual} = p_{set} + \Delta p$$

b) Interpretation of mean pressure during burning interval.

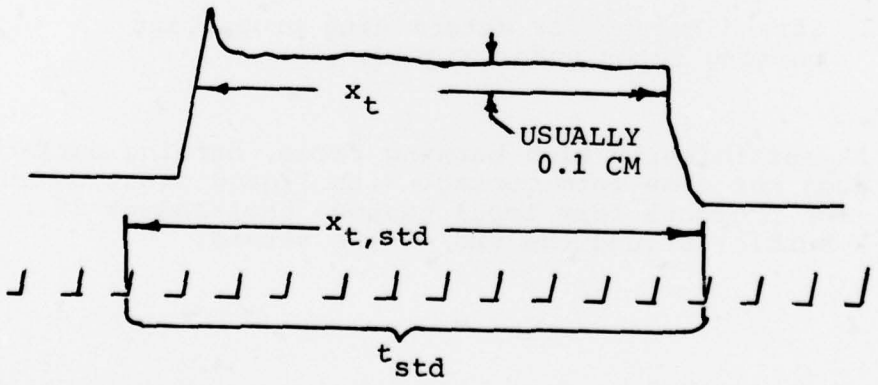

$$t_b = x_t t_{std}/x_{t,std} \quad \text{and} \quad r = L/t_b$$

c) Determination of burning time.

Fig. 3 Illustration of data records and data reduction for burning under liquid experiments.

EXPERIMENTAL ARRANGEMENT FOR OBTAINING BURNING UNDER LIQUID MOVIES

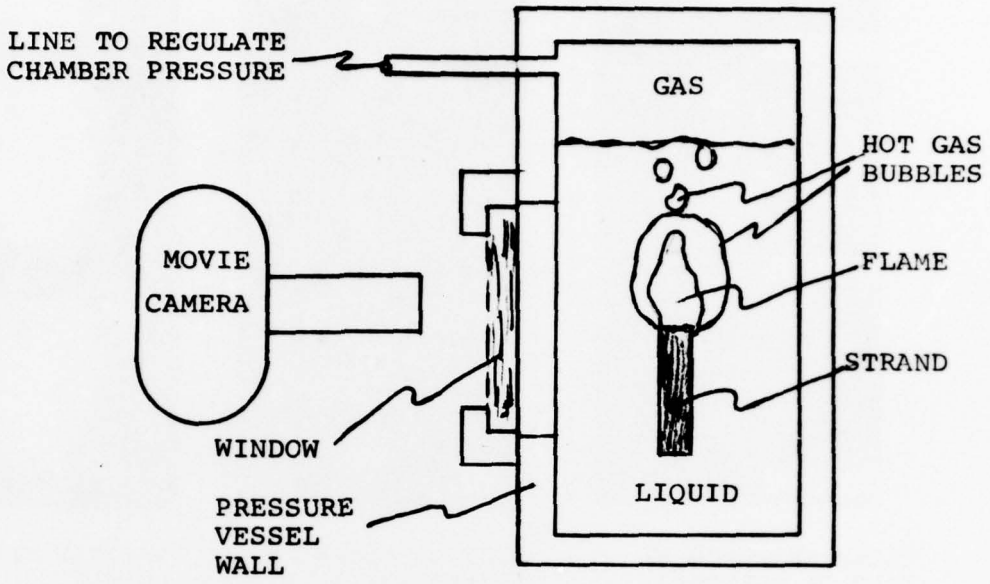

a) Side view.

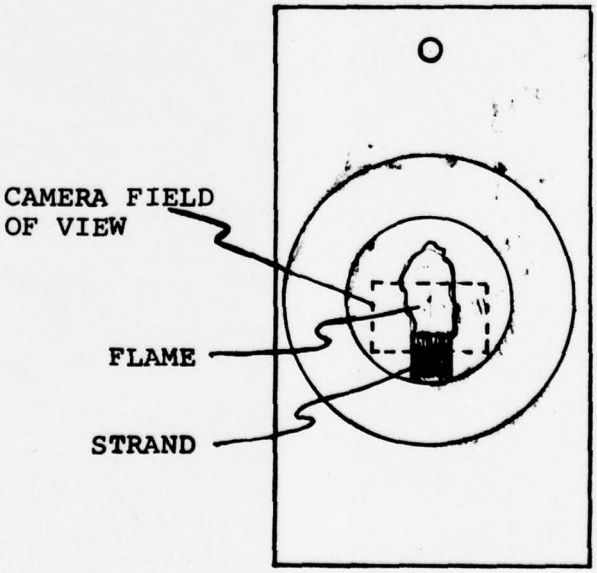

b) View through window in combustor.

Fig. 4 Experimental arrangement for obtaining burning under liquid movies.

VIEW OF STRANDS 1 MM THICK - FRAMES 0.0005 SEC APART

FLAME SHROUDED BY FILM OF QUENCHED PROPELLANT

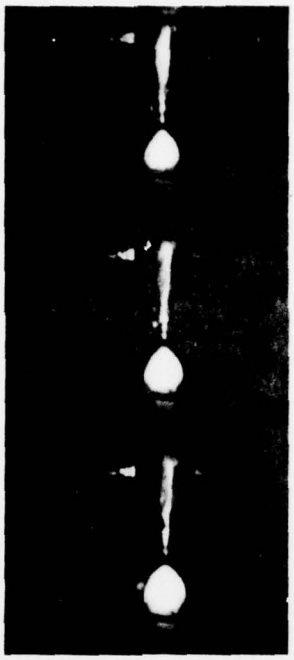

VISIBLE FLAME IN GAS POCKET IN OIL 0.3 MM ABOVE SURFACE

VISIBLE FLAME CLOSELY COUPLED TO SURFACE

COMBUSTION GASES ISSUING THROUGH FILM OF QUENCHED PROPELLANT

FLAME IN GAS POCKET IN OIL 5 MM ABOVE SURFACE

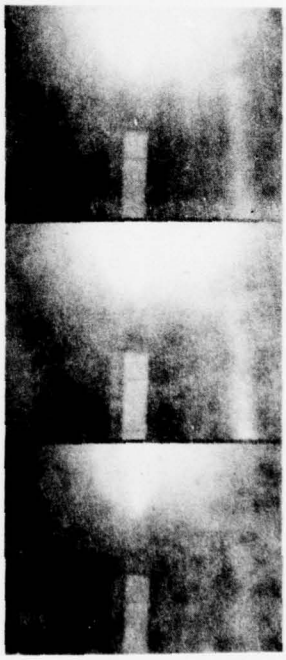

VISIBLE FLAME ABOUT 2.5 MM ABOVE SURFACE

Fig. 5 Printed frames from high speed movie (2000 fr/sec) of HEN-12 burning in H_2O oil and N_2 showing how gas pocket and film of quenched propellant isolates surface from surrounding liquid.

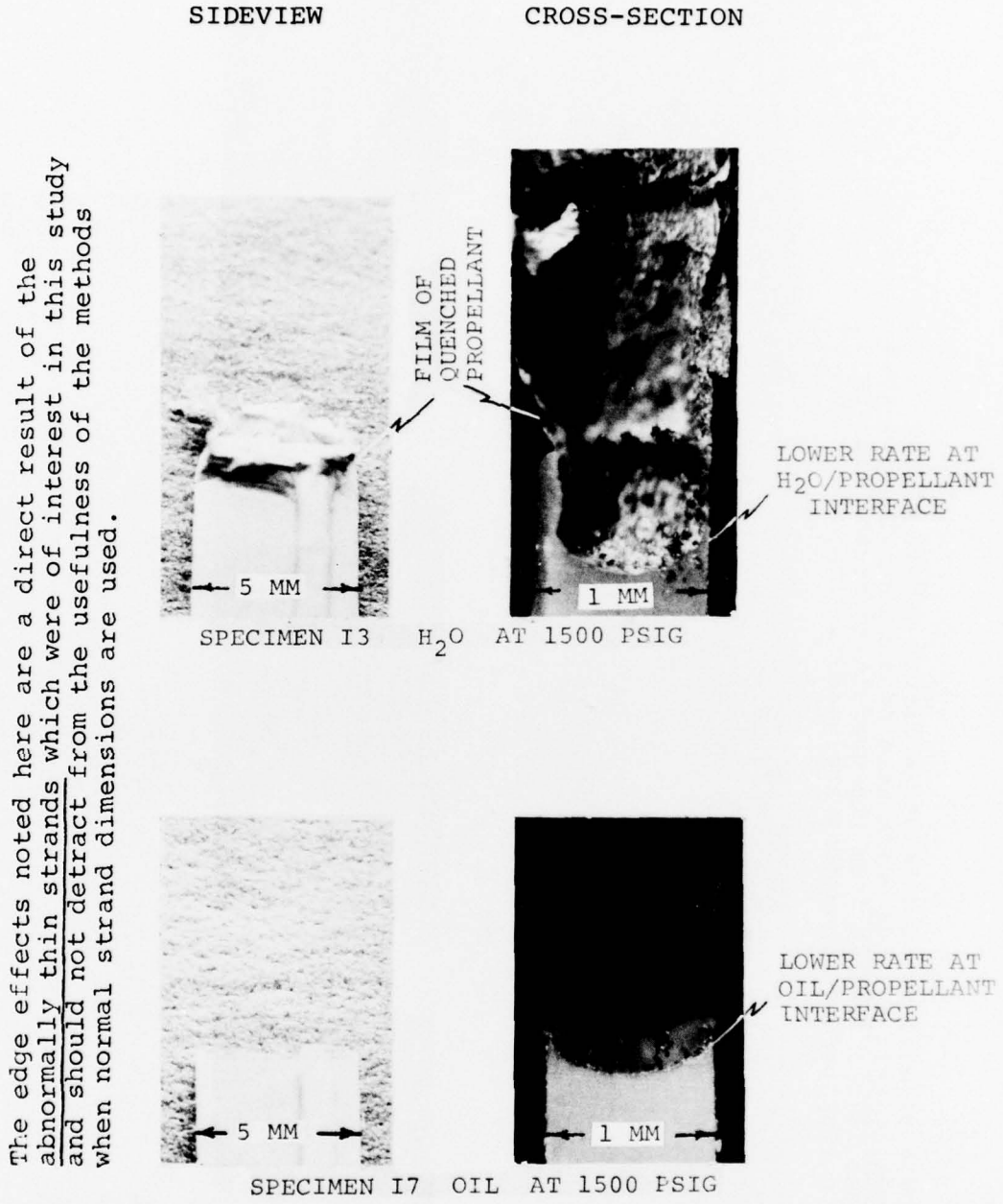

Fig. 6 Photographs of extinguished HEN-12 showing that liquid adjacent to burning surfaces significantly lowers the burning surface.

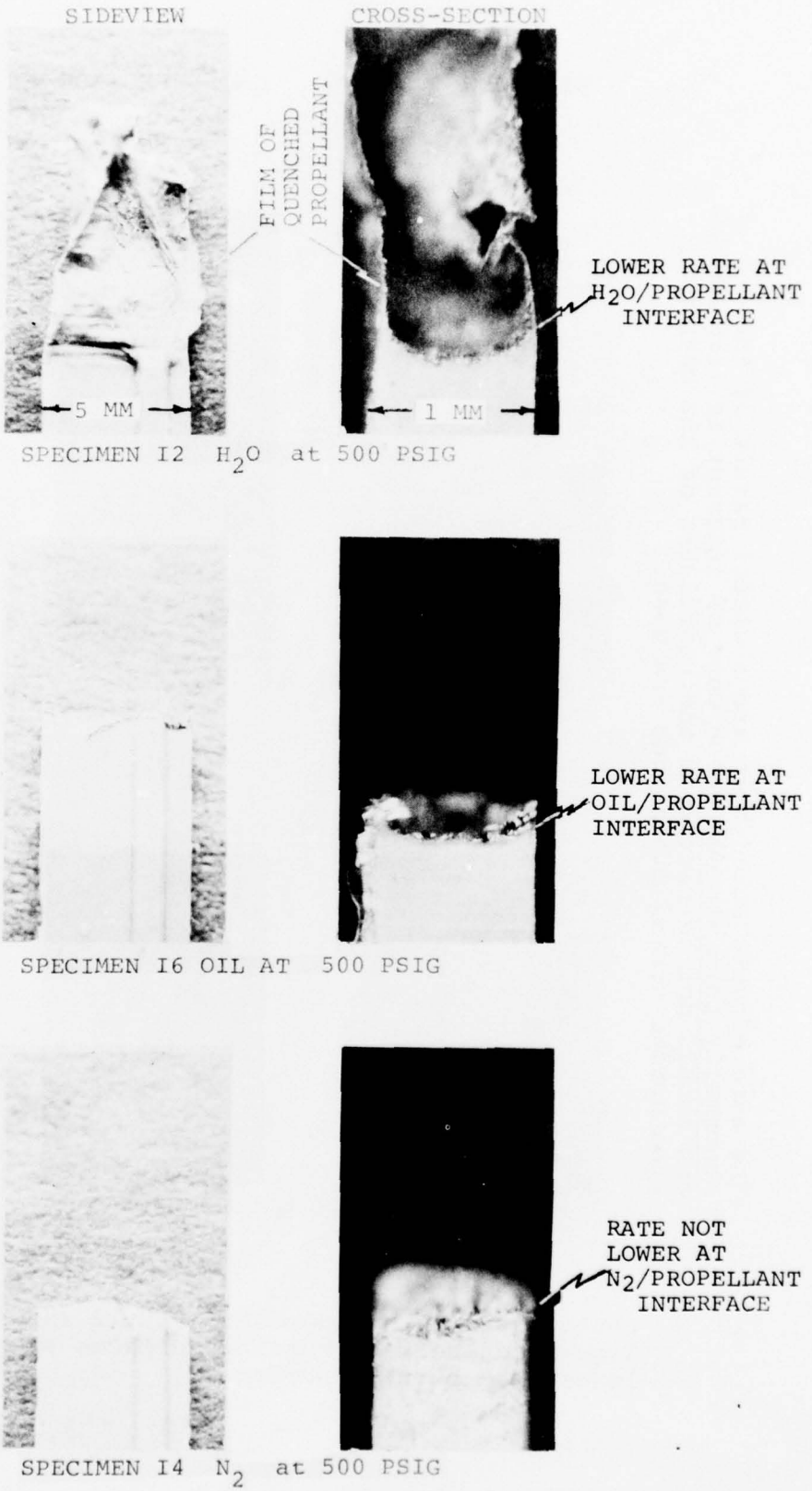

The edge effects noted here are a direct result of the abnormally thin strands which were of interest in this study and should not detract from the usefulness of the methods when normal strand dimensions are used.

Fig. 7 Photographs of extinguished HEN-12 showing that liquid adjacent to burning surfaces significantly lowers the burning rate (500 psig).

$$\hat{t} = a_0 + a_1 x$$

$$r = dt/dt = 1/a_1.$$

	SPEC.	$\bar{p}$ PSIG	T_0 °F	dx/dt in/sec	c_d	$s_{t \cdot x}$ SEC
GOOD DATA	10	509	87	0.820	0.99995	0.010
	14	1038	88	1.123	0.99989	0.011
	13	1568	90	1.360	0.99980	0.012
DATA WITH SCATTER	6	1546	80	1.212	0.99956	0.020

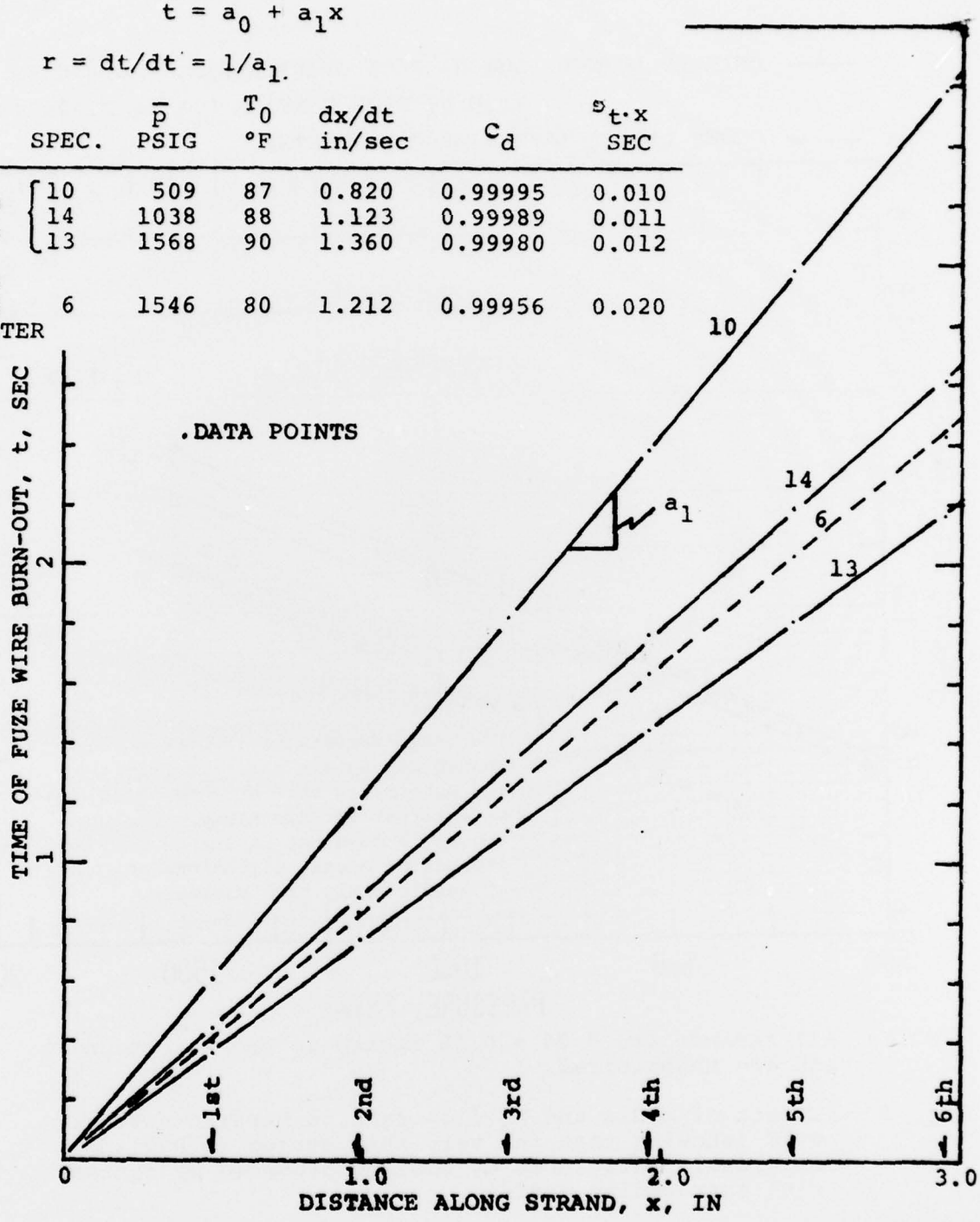

Fig. 8 Time to burn through individual breakwires and linear regression least square fit through x, t points.

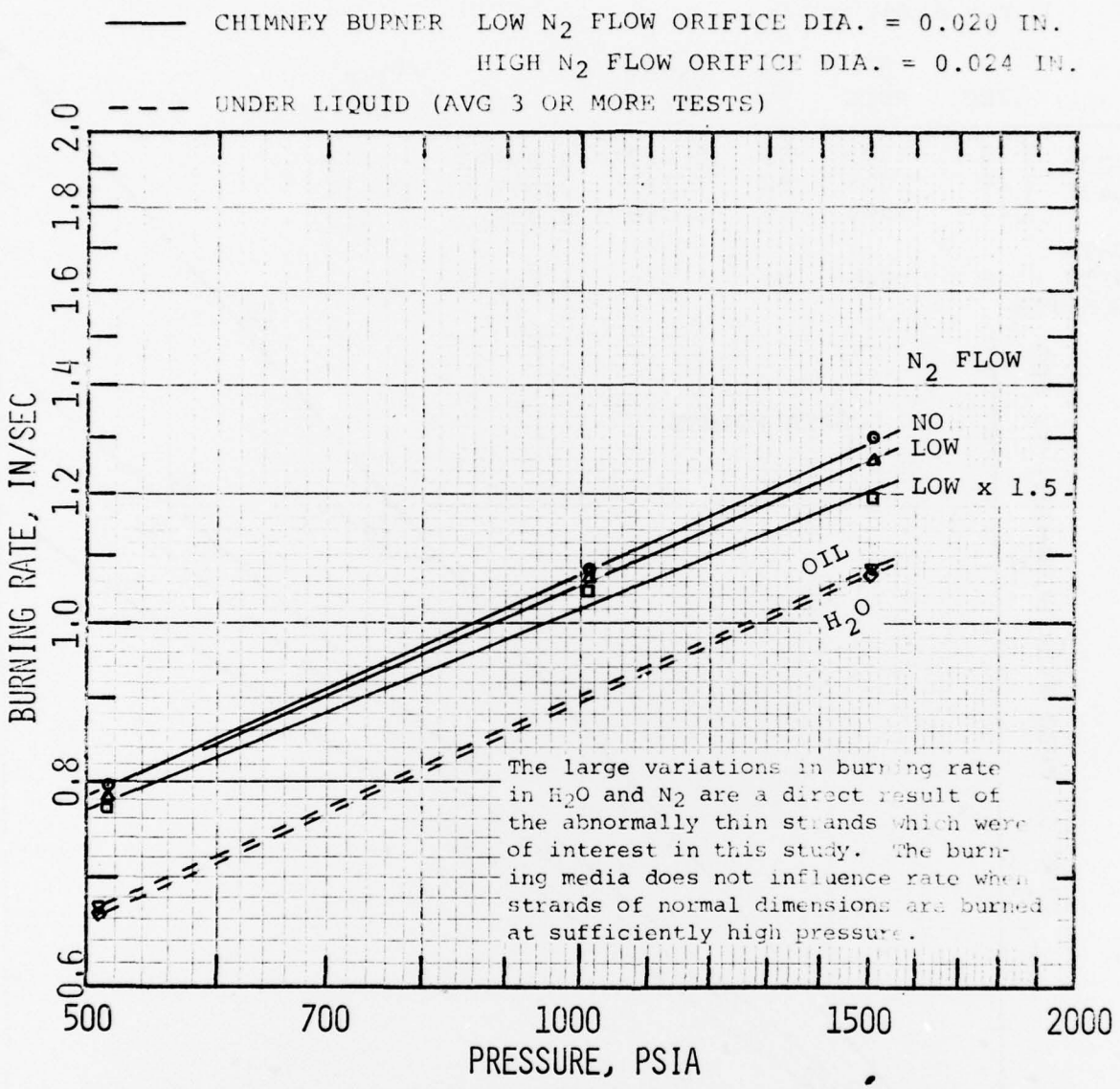

NOTE: All strands are 0.04 x 0.18 inches in cross-section and are uninhibited.

Fig. 9 Effect of media and N_2 flow rate on burning rate at 80°F [showing that the very thin strand (0.040 in.) is greatly influenced by cooling produced by contact with surrounding media].

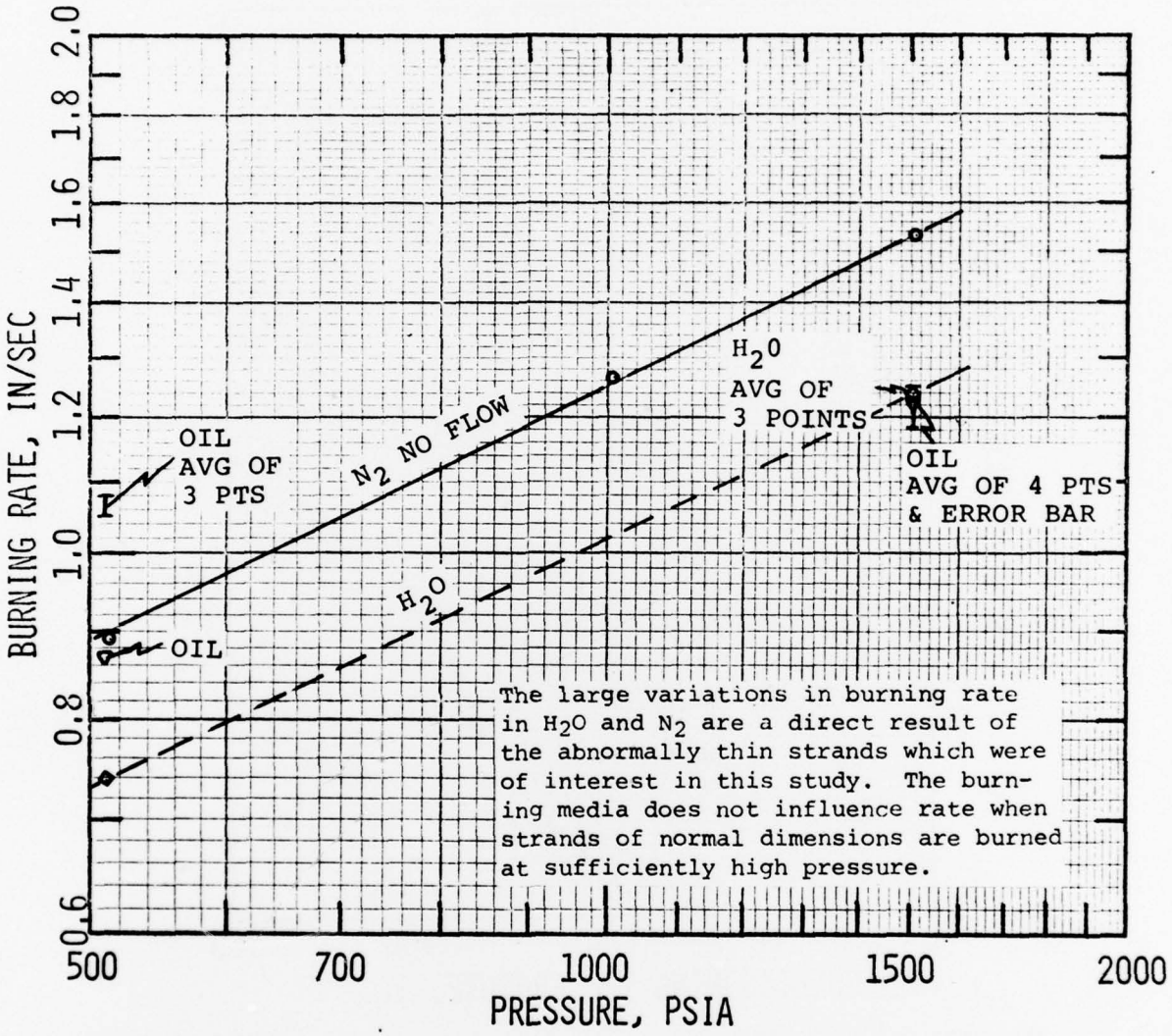

Fig. 10 Effect of media on burning rate at 140°F [showing that burning under oil produces erratic results (at 500 psi) which probably results from secondary reactions between the oil vapors and the propellant combustion products].

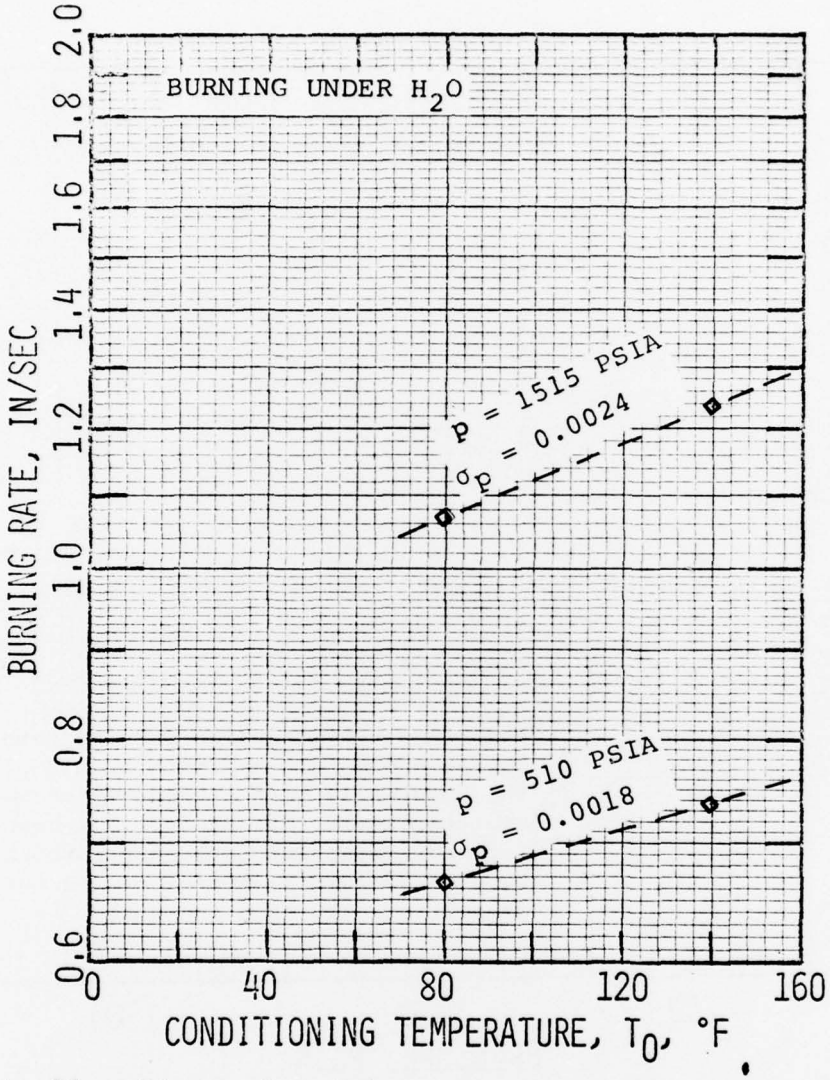

Fig.11 Effect of initial temperature on burning rate (r vs T_0 with p as a parameter) under H_2O.

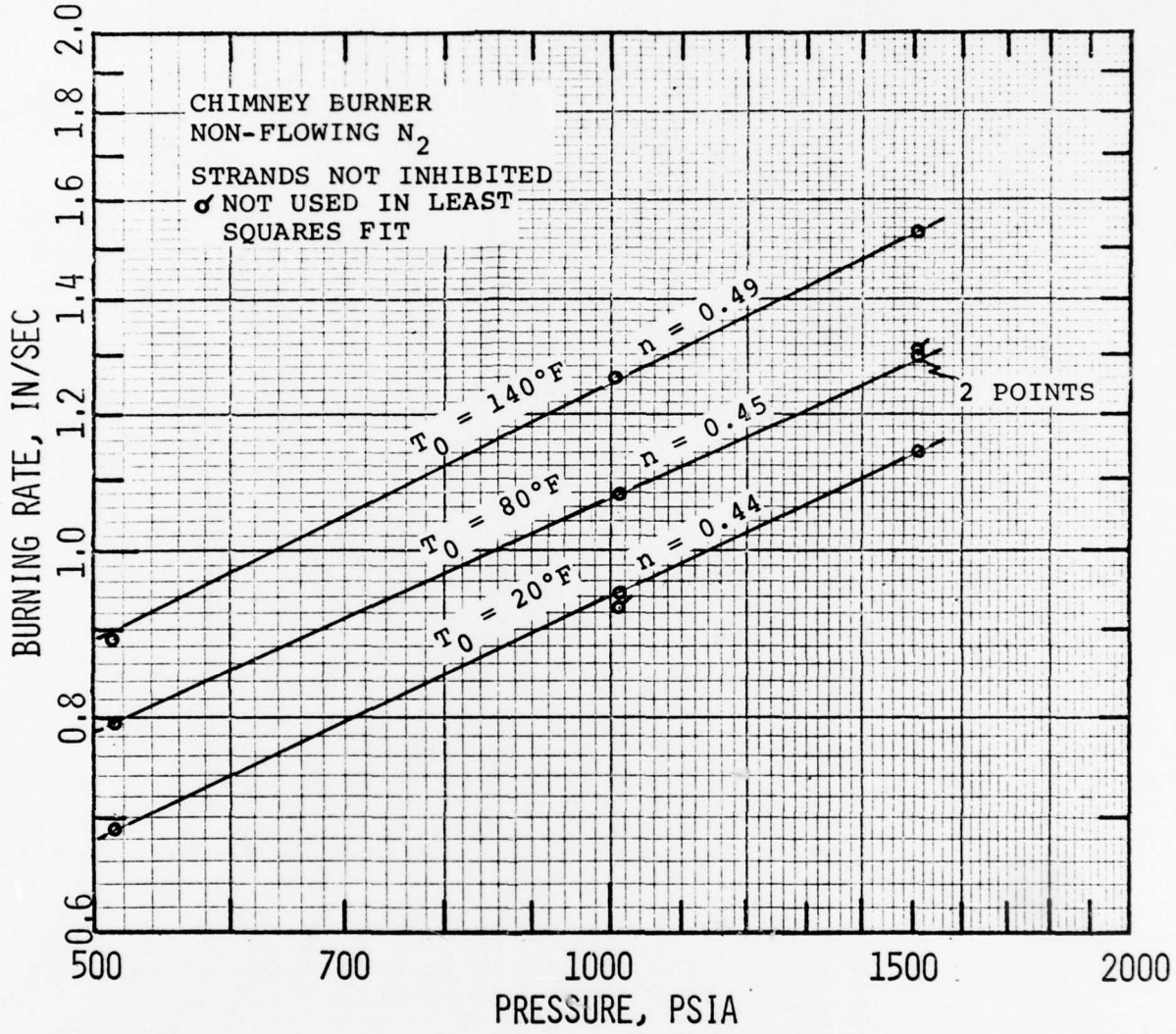

Fig. 12 Effect of initial temperature on burning rate (r vs p with T_0 as a parameter) in nonflowing N_2.

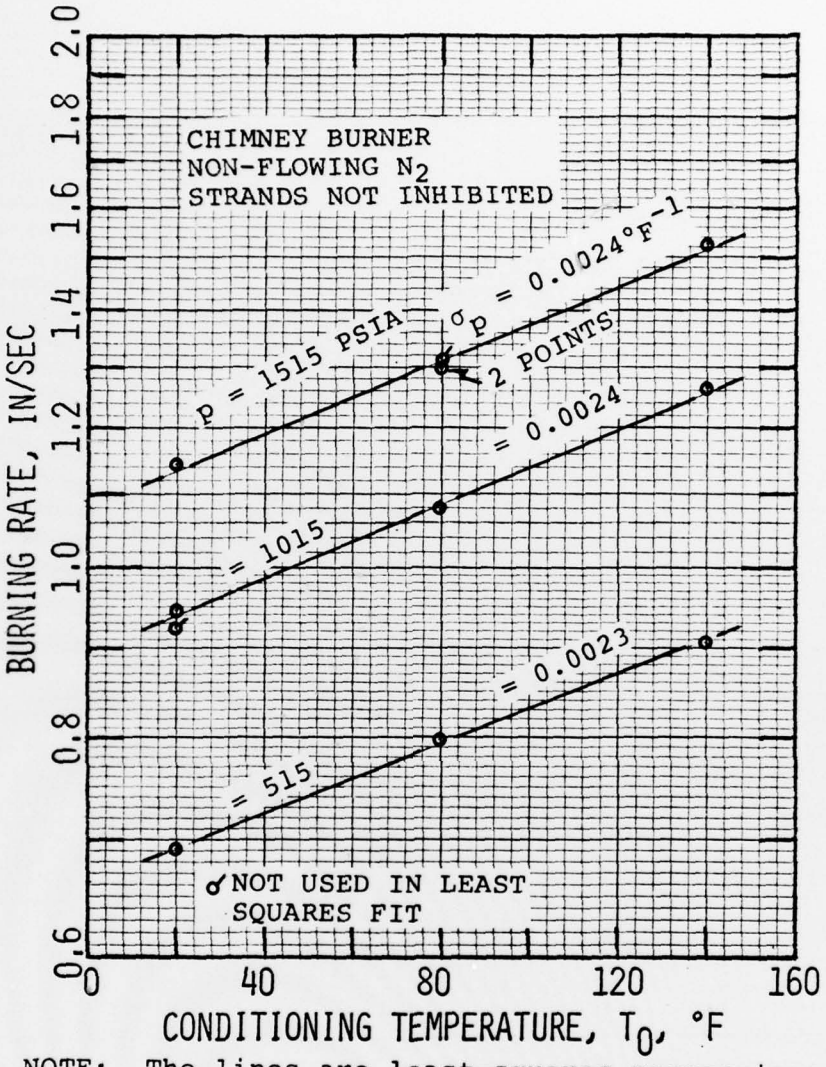

NOTE: The lines are least-squares regressions through the 20, 80 and 140°F points.

Fig. 13 Effect of initial temperature on burning rate (r vs T_0 with p as a parameter) in non-flowing N_2.

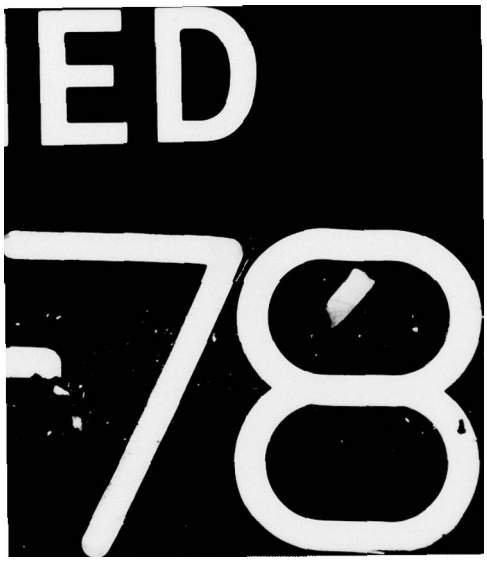
ED
78